12-2016

Design, Modeling and Simulation of a Thermoelectric Cooling System (TEC)

Pooja Iyer Mani
Western Michigan University, poojaiyer2709@gmail.com

DESIGN, MODELING AND SIMULATION OF A THERMOELECTRIC COOLING SYSTEM (TEC)

by

Pooja Iyer Mani

A thesis submitted to the Graduate College
in partial fulfillment of the requirements
for the degree of Master of Science in Engineering (Mechanical)
Mechanical and Aerospace Engineering
Western Michigan University
December 2016

Thesis Committee:

HoSung Lee, Ph.D., Chair
Muralidhar Ghantasala, Ph.D.
Chris Cho, Ph.D.

DESIGN, MODELING AND SIMULATION OF A THERMOELECTRIC COOLING SYSTEM (TEC)

Pooja Iyer Mani, M.S.E.

Western Michigan University, 2016

Thermoelectric Devices are solid state devices which directly convert thermal energy to electrical energy and vice versa. In the recent past, a lot of effort has been made to improve the performance and also the power generated by a thermoelectric device. This is done by attaching heat sinks on either sides of the device. Optimizing heat sinks improves the overall efficiency of it but on the other hand the device also has to be optimized. TECs are mostly used for electronic cooling where the heated electronic devices serve as target that needs to be cooled while air acts as a heat sink with natural convection. In this project, maximizing the cooling power of a TEC has be studied and its effect with respect to variations in the TE geometry has been discussed. 1D analytical model has been developed using Mathcad and a 3D model of the same has been numerically simulated using ANSYS whose setup used has been explained in details. At low leg length of the TEC's, the cooling power can be improved but a lot of other parameters have to be taken into account to accurately model the system. The contact materials used to electrically connect the device and the resistance of the conductor play a very important role while calculating the cooling power at low leg lengths and hence cannot be neglected. Results show that cooling power of the TEC can be dramatically improved at low leg lengths and with better heat sink material.

ACKNOWLEDGEMENTS

I would like to thank my advisor Dr. HoSung Lee for his encouragement for my work. This work would not have been possible without his support and guidance. It has been a pleasure working with him and learning everything he has taught us.

I would also like to extend my thanks to my committee members, Dr. Muralidhar Ghantasala and Dr. Chris Cho, for their guidance and suggestions to improve the quality of this work.

I would also like to thank my family, my mother, my father, and my brother for their support and trust they had placed in me. Their belief in me is a big part of my accomplishment.

Last but not the least, I would like to thank my friends who believed in me and supported me throughout my work with this project.

Pooja Iyer Mani

TABLE OF CONTENTS

Table of Contents - Continued

LIST OF TABLES

LIST OF FIGURES

List of Figures – Continued

NOMENCLATURE

A_c	total fin surface area cold side heat sink (mm^2)
A_e	cross-sectional area of thermoelement (mm^2)
A_h	total fin surface area hot side heat sink (mm^2)
A_M	base area of thermoelectric module (mm^2)
COP	the coefficient of performance
c_p	specific heat (J/kg.K)
G_e	thermocouple geometric ratio
H	total height of thermoelectric air conditioner (mm)
h	heat transfer coefficient of the fluid (W/m^2K)
I	electric current (A)
j	unit cell number
L	total length of thermoelectric air conditioner (mm)
k	thermoelement thermal conductivity (W/m K), $k = k_p + k_n$
K	thermal conductance (W/K), $K = kA_e/L_e$
L_e	length of thermoelement (mm)
n	the number of thermocouples
N_k	dimensionless thermal conductance, $N_k = n(A_e k/L_e)/\eta_h h_h A_h$
N_h	dimensionless convection, $N_h = \eta_c h_c A_c/\eta_h h_h A_h$

N_I dimensionless current, $N_I = \alpha I/(A_e k/L_e)$

P_{in} input power (W)

q_x the rate of heat transfer around the differential element

$\dot{Q}$ the rate of heat transfer

$\dot{Q}_c$ cooling capacity (W)

$\dot{Q}_h$ heat rejection (W)

R_{Al} thermal resistance of the aluminum block

t_{al} thickness of the aluminum block

T_c cold junction temperature (°C)

T_h hot junction temperature (°C)

$T_{\infty c}$ cold fluid temperature (°C)

$T_{\infty h}$ hot fluid temperature (°C)

$\dot{V}_c$ cold fluid volume flow rate (CFM)

$\dot{V}_h$ hot fluid volume flow rate (CFM)

W total width of thermoelectric air conditioner (mm)

$\dot{W}$ electrical power (W)

x direction along the length of the element

Z the figure of merit (1/K) $= \alpha^2/\rho k$

Greek symbols

α Seebeck coefficient (V/K), $\alpha = \alpha_p - \alpha_n$

ρ electrical resistivity (Ω cm), $\rho = \rho_p + \rho_n$

φ alimunum block thermal resistance (K/W)

η fin efficiency of the heat sink

γ thermal resistances ratio between the heat sink and aluminum block

Subscripts

al aluminum

c cold

ct contact

e thermoelement

h hot

in inlet

j unit cell number

m measured

n n-type element

no	the number of thermocouples
out	outlet
opt.	optimal quantity
p	p-type element
$*$	dimensionless
∞	fluid

1 Introduction

Thermoelectrics is defined as the generation of electricity from a given temperature difference or vice versa. Solid state devices capable of producing power, these devices are environment friendly that come with low maintenance and reliability. They use a very simple concept of running on a temperature difference and as long as this criteria is being fulfilled, energy is produced. The concept of thermoelectricity can be classified into 2 parts. Thermoelectric Coolers (TEC) and Thermoelectric Generators (TEG). In order to run a TEC, a certain amount of current has to be input along with maintaining a temperature difference which gives a cooling power and the coefficient of performance of the device can then be measured. However, in a TEG, a load resistance is input along with maintaining a temperature difference and electricity is thus generated from these conditions. There have been quite a few number of applications in the recent past and the number of applications are increasing with time. Thermoelectrics has found its way into air conditioning systems, automobile applications, solar energy applications and many others.

1.1 History and Derivation of Thermoelectrics

Early years of 19^{th} century, paved way for the discovery of the concept of Thermoelectricity. In 1821, Thomas Seebeck discovered that an electromotive force could be generated when a circuit was made out of two dissimilar materials and when the junction was heated. The electromotive force that was generated was named the Seebeck Effect. A few years later, Jean Peltier discovered that this same

process could be reversed to produce heat when voltage was applied across the junction of two dissimilar materials [1]. In short, when current is passed through a circuit, one junction increases in temperature while the other junction cools down. A thermoelectric module is formed when a number of dissimilar materials are connected thermally in series and electrically parallel to each other [2].

At the end of the 19th century, electrons were discovered. And that was when the concept of thermoelectricity came to be clearer to the people working on it. We now understand that electrons can be liberated from any source even at temperatures as low as the room temperature. This is the reason we have electrostatics everywhere [1]. When a temperature difference is applied across a conductor, the hot region liberates more electrons and diffusion takes place from the hot side to the cold side. This distribution of electrons provoke the generation of an electric field which helps the electrons move from the hot side to the cold side due to Coulomb force. Therefore an electromotive force (emf) is generated which causes the current to move in the direction opposite to the flow of temperature. The same can be said about the opposite criteria as well. The movement of electrons due to the application of a current results in the generation of temperature difference. This concept is shown in the following figure.

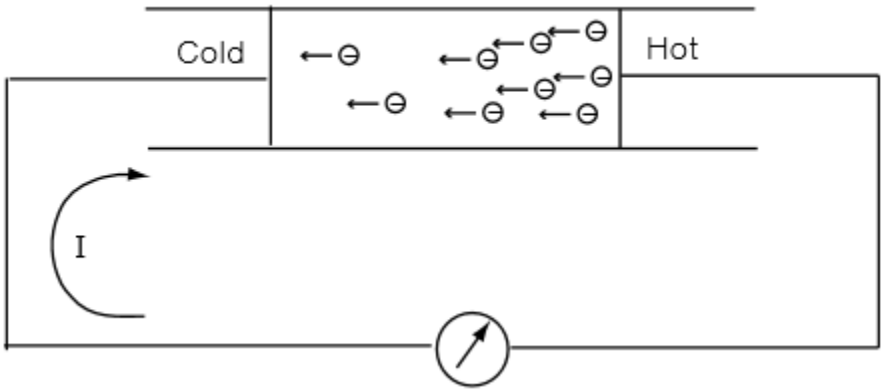

Figure 1.1 Movements of electrons in a thermoelectric material

1.2 The Seebeck Effect

When there is a temperature difference in a thermoelectric material, an electric current is created due to movement of holes and electrons in the semiconductor materials. The effect that causes this behavior is called the Seebeck Effect. [3]

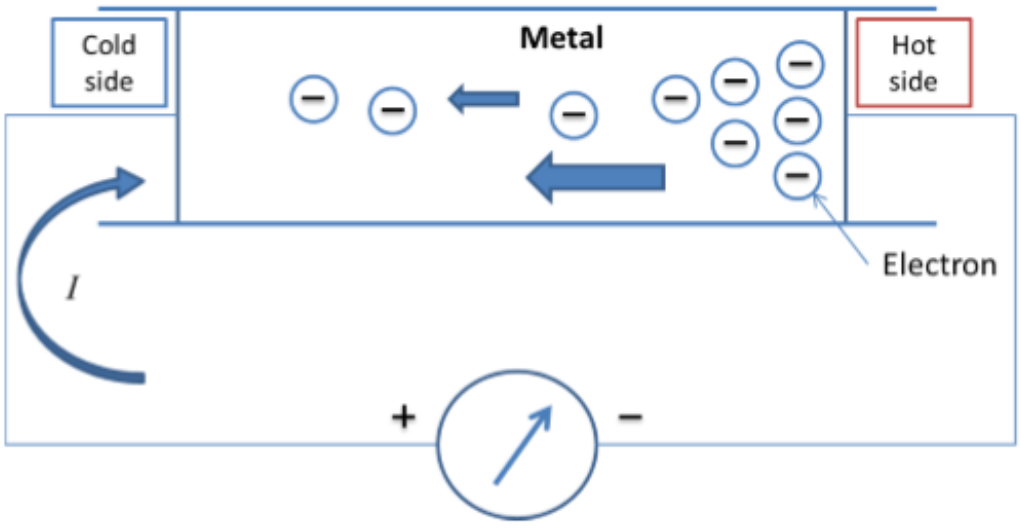

(a)

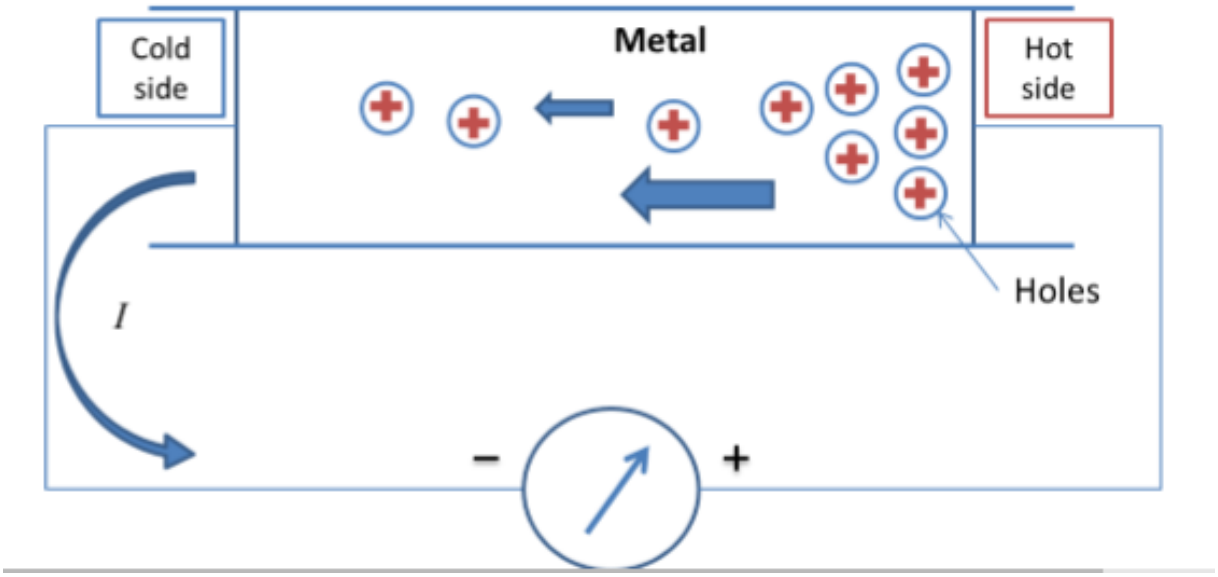

Figure 1.2 The movement of (a) holes (b) electrons in the Seebeck Effect

A potential difference is developed when a voltmeter is placed in between the cold side and the hot side. This potential difference is proportional to the temperature difference between these sides. This relation is written as,

$$V = \alpha \Delta T \qquad 1.1$$

α is the Seebeck Coefficient while ΔT is the temperature difference between the two sides of the thermoelectric material. Hence, in a given thermoelectric module, α and ΔT are the factors that determine the voltage across it and depending on the resistance of the material and its geometry, the current can be determined [3].

1.3 The Peltier Effect

Heat must be continuously added to or rejected from the body in order to keep the junction temperatures constant when there is a current passing through it. The total

amount of heat added or rejected is proportional to the amount of current supplied. This phenomenon is called the Peltier effect and can be defined using the following equation.

$$Q_{peltier}=\Pi_{AB}I \qquad 1.2$$

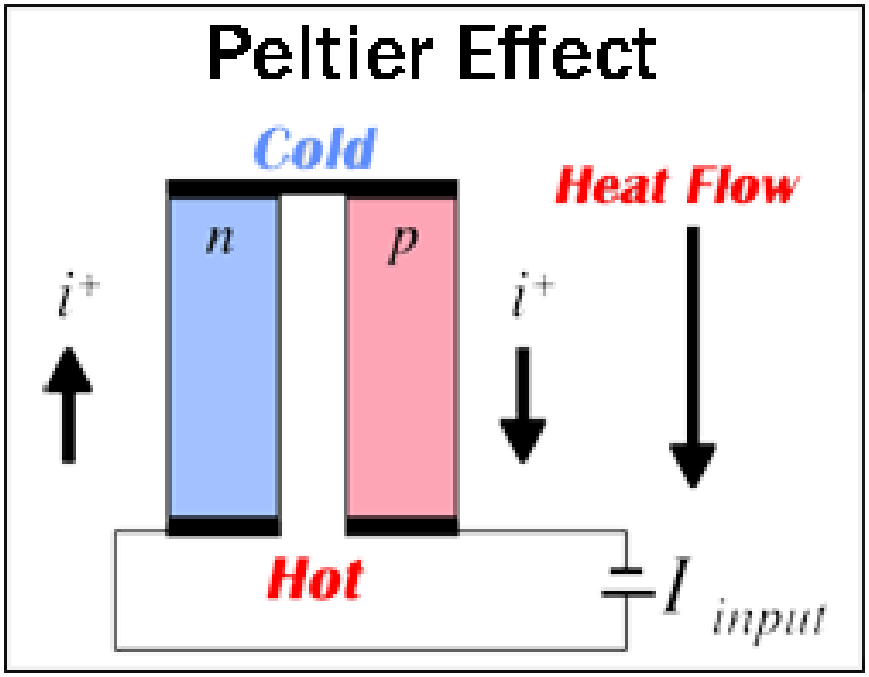

Figure 1.3 The Peltier Effect

Here, Π_{AB} is the Peltier coefficient, $Q_{peltier}$ is the total heat added or rejected by the system and I is the current passing through the thermoelectric element [3]

1.4 The Thomson Effect

For the most part, the Thomson Effect is very similar to the Peltier Effect. Major difference between the two lies in the fact that the Thomson Effect requires a temperature gradient across the semi-conductor element along with the current supplied. This means that when current is supplied and when there is a temperature

gradient along the length of the thermoelectric element, heat is either absorbed or rejected depending on the direction of the current supplied. Hence, the Thomson Effect is proportional to the supplied current and the temperature gradient. It can be defined using the equation; [3] [4] [5] [2] [6]

$$Q_{Thomson}=\tau I \Delta T \qquad 1.3$$

τ is the Thomson Coefficient in the above equation.

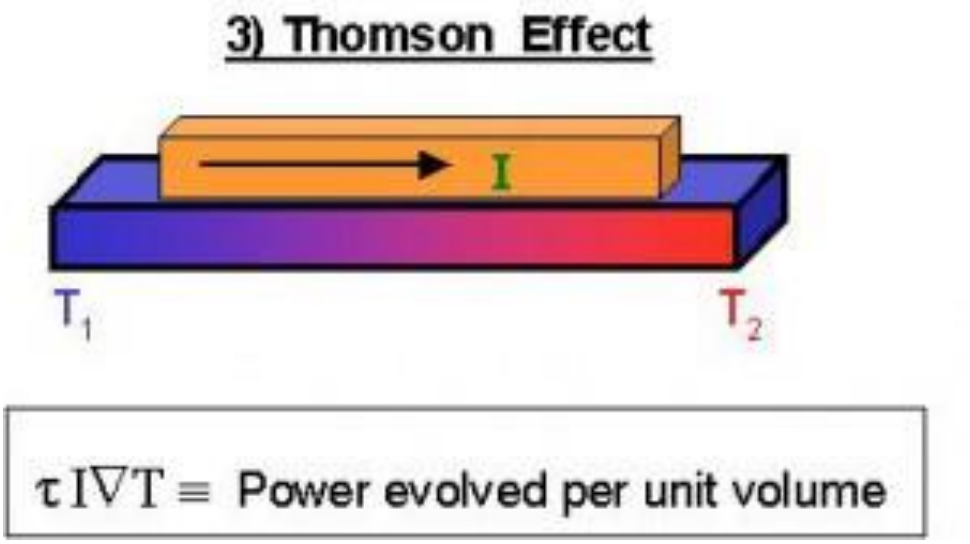

Figure 1.4 The Thomson Effect

1.5 Figure of Merit

Figure of merit is a term used to define the performance of a thermoelectric device. It can be calculated using the equation;

$$Z = \frac{\alpha^2}{\rho k} = \frac{\alpha^2\,\sigma}{k} \qquad 1.4$$

where α is the Seebeck coefficient in (V/K) , ρ is the electrical resistivity in (Ωm), k is the thermal conductivity in (W/mK) and σ is the electrical conductivity in (mK/W).

The dimensionless figure of merit is defined as ZT where T is the absolute temperature. For a long time, the value of ZT had been constrained to 1. But recent innovations have proven to have a ZT value greater than 1 that defines the performance of a thermoelectric system. The higher the value of ZT, higher the energy conversion efficiency of the device. From equation (1.4), the interdependence of the parameters is very evident. In order for the figure of merit to be high, the Seebeck coefficient α and the electrical conductivity σ must be high while the thermal conductivity k must be low. The values of these parameters are the defining points in the performance of a thermoelectric system and it has been very difficult to model a device that satisfies this interdependence completely.

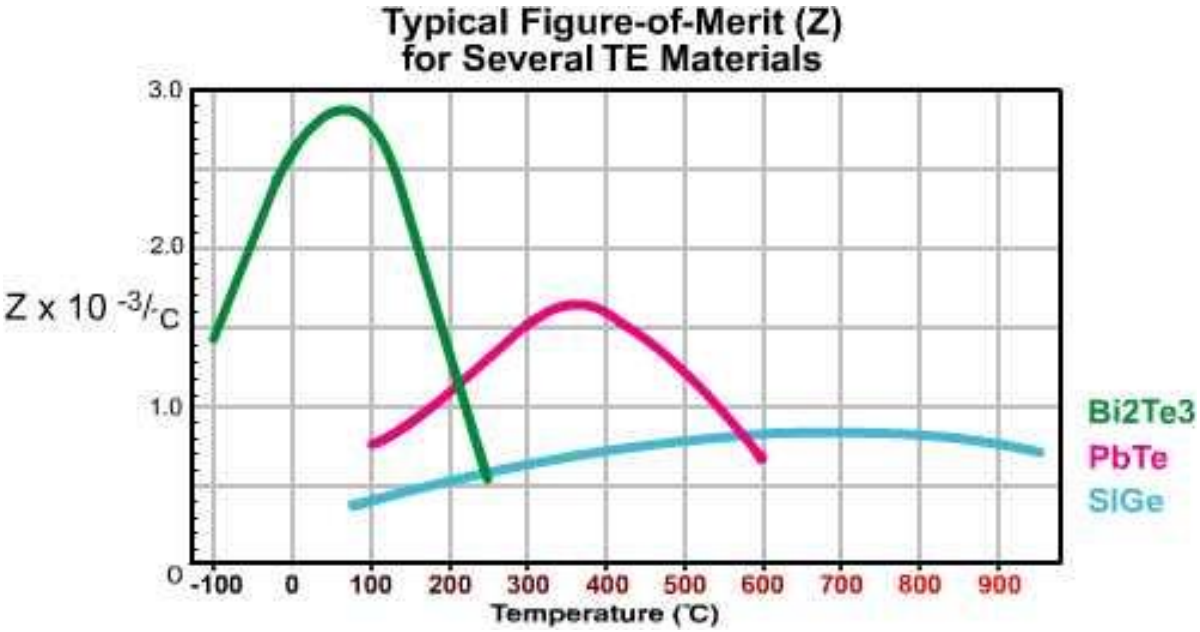

Figure 1.5 Figure of merit vs temperature for typical thermoelectric structures

1.6 The Thermoelectric Module

A thermoelectric pair consists of a p-type semiconductor, n-type semiconductor, and copper to connect the semiconductors. A module however, consists of a number of thermoelectric pairs depending on the application. The most widely used semiconductor is Bismuth Telluride. In the recent past however, materials better than Bismuth Telluride have been discovered. Materials like skutterudite have proven to give better results under certain conditions. Depending on whether the module is a thermoelectric cooler or a generator, electric current is either supplied or generated from the system. In a thermoelectric cooler, the main focus of the current work, when an electric current is supplied to the n-type semiconductor, heat is absorbed and hence transported to the hot side. Thereby given an overall cooling effect. When current is applied in the opposite direction, an opposite effect is seen

and the module gives a heating effect [6]. This concept holds an advantage of application over commercial refrigerators and heat pumps where these possess the advantage of direct energy conversion, high reliability, low maintenance, no refrigerants and all these advantages stand true mainly because the thermoelectric cooler is a solid state device [7] [6].

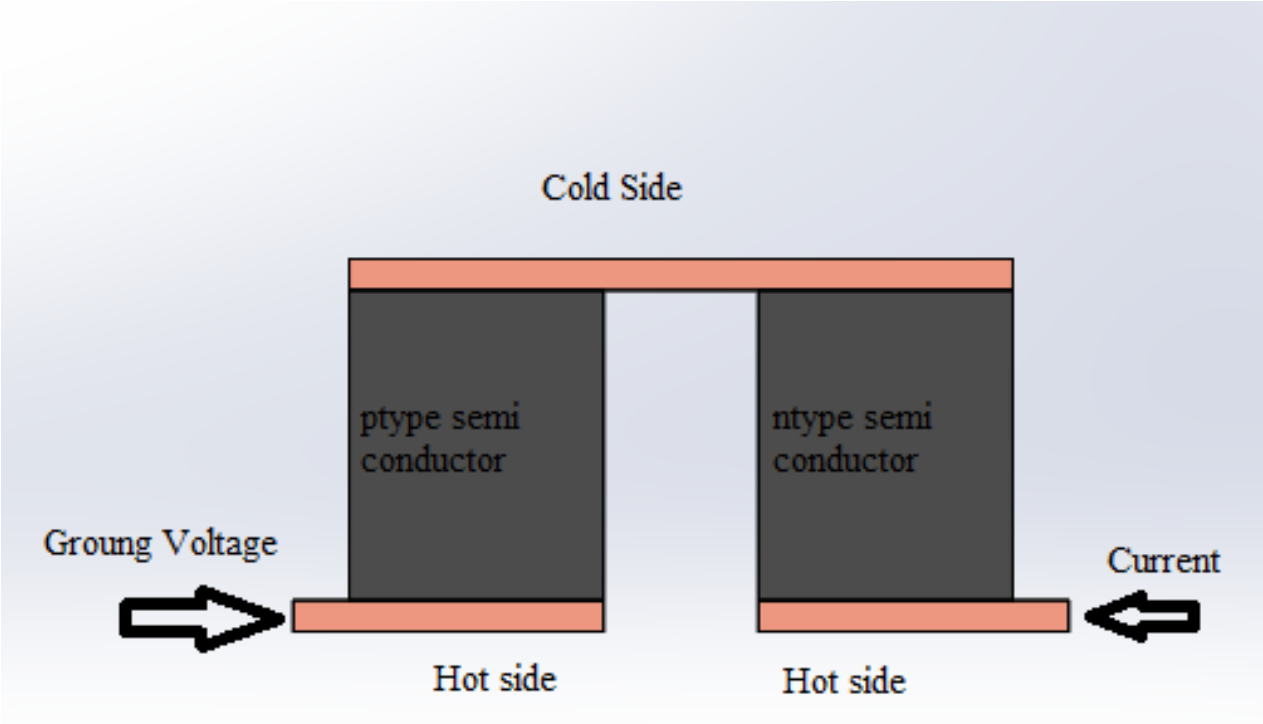

Figure 1.6 Thermocouple

2 Thermoelectric Cooling and its Background

Thermoelectric devices are devices of the future. The applications of thermoelectric cooling devices have so far been employed in a lot of devices where the size of the device is small. In applications where the temperature needs to be stabilized, a cooling effect needs to be produced or heat up the device using a reverse current, thermoelectric cooling modules have been used. Peltier models have also been used in many everyday life situations like cool storage boxes for medicine or for cooling boxes for picnic storage [8].

Some of the most recent applications in the concept of thermoelectric cooling is in vehicle air conditioning. Almost 10% of the annual consumption of fuel can be directed to the use of air conditioning [3]. Most of these use refrigerants like R-134a which has adverse effects on the environment being a major greenhouse gas. There is a lot of debate in the current day about banning all the environment depleting compounds and R-134a is definitely one of them. [9]. The U.S. Department of Energy (DOE) and the California Energy Commission funded a project to research an application involving thermoelectric heat ventilating and air conditioning system (TE HVAC) that promised to replace the traditional air conditioning systems in vehicles [3] [10]. Use of a thermoelectric air conditioning system (TEAC) in place of the traditional air conditioning system has been proven to have benefits such as being able to produce a cooling effect without the use of environment depleting substance like the R-134 and also having a scope to select the areas needing heating or cooling instead of randomly cooling the whole area

which in turn reduces the amount of fuel consumed considerably hence also reducing the exhaust [3].

2.1 Thermoelectrics Today

Although the concept of thermoelectrics was observed centuries ago, the first model of its kind had come out only in the recent times. The first ever functioning device was developed in the late 1950s. These are also known as the first generation thermoelectric devices. After a lot of questioning, answering and debating, many theories had been developed on various genres of this concept. Some of them included the study of thermoelectric properties with reduction in size. Early 90s saw the rise of experimental research that eventually gave several advances in the early 21st century.

Nano material have been discovered to have an effect on the value of the figure of merit that is worth noting. Due to an inverse relation between all the three parameters linking the figure of merit, it becomes more difficult to model a device that agrees to produce a higher value of ZT. Hence, the lattice thermal conductivity of the material was taken advantage of because this is the only parameter that seems independent of the electronic structure of the model.

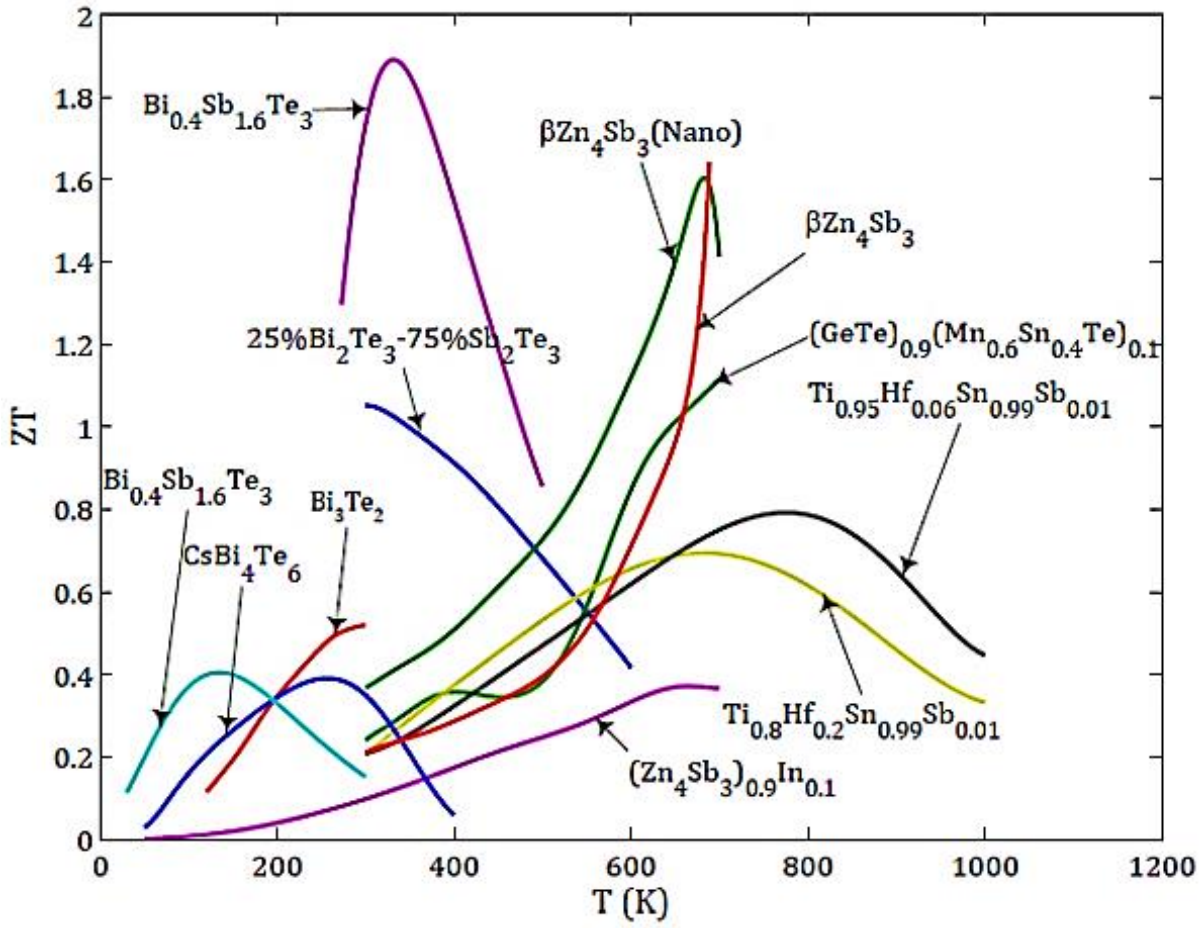

Figure 2.1 Dimensionless ZT vs T of different thermoelectric compounds

2.2 Thermoelectric Ideal (standard) Equations

2.2.1 General governing equations

Considering a non-uniformly heated thermoelectric material for isotropic material properties, the continuity equation is given as

$$\vec{\nabla} \cdot \vec{j} = 0 \qquad 2.1$$

Where $\vec{\nabla}$ is the differential operator along with respect to length and $\vec{j}$ is the current density. The electric field $\vec{E}$ is affected by $\vec{j}$ and the temperature gradient $\vec{\nabla}T$. The coefficients have contributions from both Ohm's law and the Seebeck effect. By differentiating Eq. (2.1) With respect to length, the electric field is equal to

$$\vec{E} = \vec{j}\,\rho + \alpha\,\vec{\nabla}T \tag{2.2}$$

The heat flow density vector (heat flux) is given by

$$\vec{q} = \alpha\,T\,\vec{j} - k\,\vec{\nabla}\,T \tag{2.3}$$

The general heat diffusion equation is expressed as

$$-\vec{\nabla}\cdot\vec{q} + \dot{q} = \rho c_p \frac{\partial T}{\partial t} \tag{2.4}$$

Here, $\dot{q}$ is the generated heat by unit volume, ρ is the mass density, c_p is the specific heat and $\frac{\partial T}{\partial t}$ is the rate of change temperature with respect to time.

For steady state Eq. (2.3) reduced to

$$-\vec{\nabla}\cdot\vec{q} + \dot{q} = 0 \tag{2.5}$$

Where $\dot{q}$ is defined as

$$\dot{q} = \vec{E}\cdot\vec{j} = J^2\rho + \vec{j}\cdot\alpha\vec{\nabla}T \tag{2.6}$$

Following equation can be obtained by substituting Eqns. (2.3) and (2.6) in equation (2.5).

$$\vec{\nabla} \cdot \left(k\vec{\nabla}T\right) + J^2\rho - T\frac{d\alpha}{dT}\vec{J} \cdot \vec{\nabla}T = 0 \qquad 2.7$$

Where $\vec{\nabla} \cdot \left(k\vec{\nabla}T\right)$ is the thermal conduction, $J^2\rho$ is the Joule heating, and $T\frac{d\alpha}{dT}$ is the Thomson coefficient. A study by [11] shows a good agreement between the Thomson coefficient as a function of temperature and the exact solution that neglected the Thomson coefficient. Hence, the Thomson coefficient can be neglected $T\frac{d\alpha}{dT} = 0$.

Assumptions of thermoelectric ideal (standard) equations

Below are the important assumptions of thermoelectric ideal (standard) equations:

1) The Thomson effect is negligible. It has been proven analytically and experimentally that the Thomson effect has a very small effect on the performance of TEG and TEC.
2) The electrical and thermal resistances between ceramic plates and thermoelectric elements are negligible.
3) The convection and radiation losses are negligible.
4) The materials properties are assumed to be independent of temperature.

2.2.2 Thermoelectric couple equations

Consider two dissimilar semiconductor elements, which are sandwiched between copper conductive tabs, each element is called a thermoelectric leg or pellet, and is either p-type material (positive) or n-type material (negative). These elements are temperature independent with their material properties, which are

Seebeck coefficient (α), electrical resistivity (ρ), and thermal conductivity (k), as illustrated in Figure 2.2.

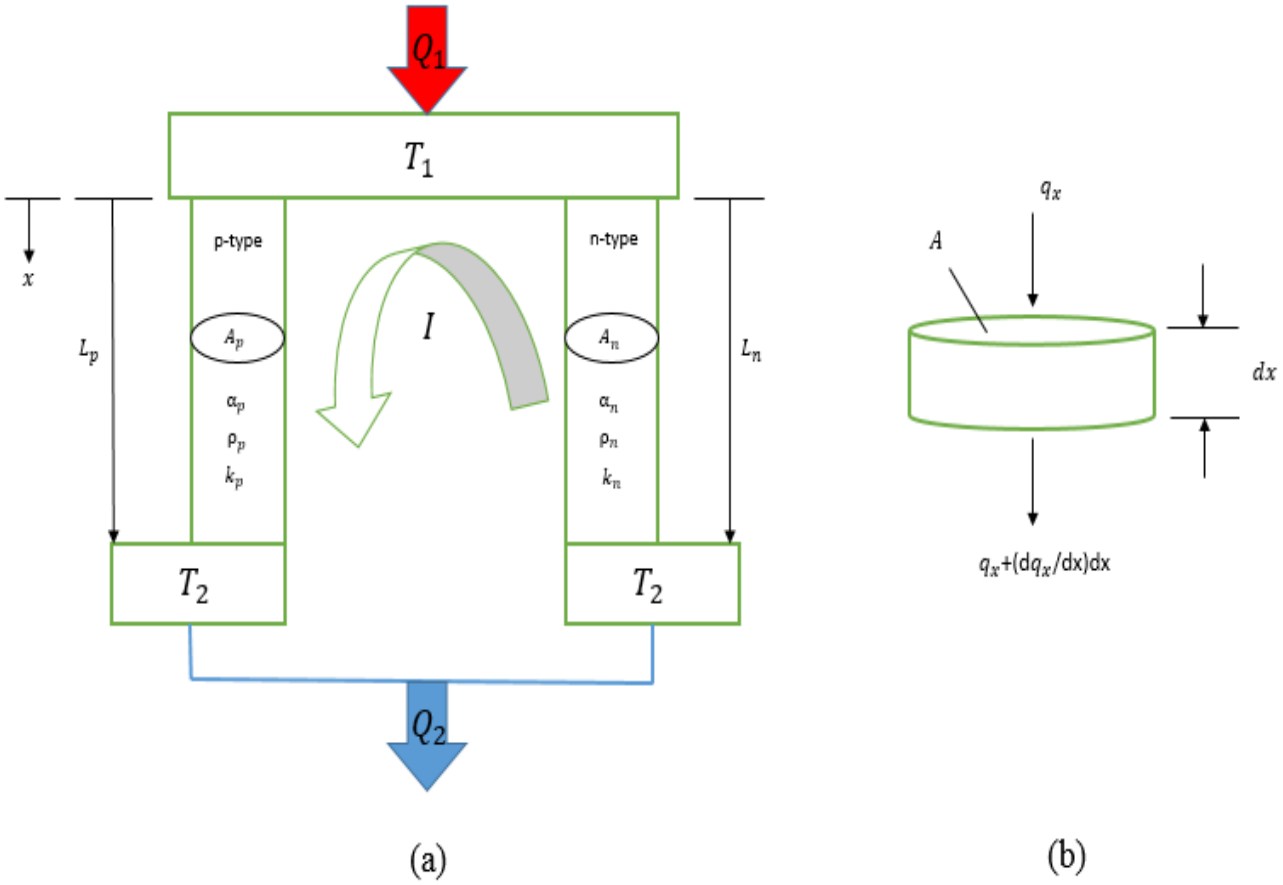

Figure 2.2 Longitudinal cross-section of a TE couple and differential element.

The steady state heat balance at T_1 becomes

$$\dot{Q}_1 = q_p + q_n \qquad 2.8$$

where q_p and q_n are the heat flows for p-type and n-type. The heat flows can be defined in terms of the Peltier heat and Fourier's law of conduction as

$$q_n = -\alpha_n T_1 I + \left(-k_n A_n \frac{dT}{dx}\Big|_{x=0}\right) \qquad 2.9$$

$$q_p = \alpha_p T_1 I + \left(-k_p A_p \left.\frac{dT}{dx}\right|_{x=0}\right) \tag{2.10}$$

By applying the heat balance on the differential element shown in Figure 2.2, the temperature gradient can be obtained as

$$\underbrace{q_x - \left(q_x + \frac{dq_x}{dx}\right)}_{\substack{\text{heat transfer} \\ \text{across the surface} \\ \text{of the element}}} dx + \underbrace{\frac{I^2 \rho_p}{A_p} dx}_{\text{Joul heating}} = 0 \tag{2.11}$$

Differentiating Eq (2.10) with respect to x gives

$$\frac{dq_p}{dx} = -k_p A_p \frac{d}{dx}\left(\frac{dT}{dx}\right) \tag{2.12}$$

Inserting Eq. (2.12) into Eq. 2.11 yields

$$-\frac{d}{dx}\left(-k_p A_p \frac{dT}{dx}\right) + \frac{I^2 \rho_p}{A_p} = 0 \tag{2.13}$$

or,

$$k_p A_p \frac{d}{dx}\left(\frac{dT}{dx}\right) = \frac{-I^2 \rho}{A_p} \tag{2.14}$$

Integrating Eq. 2.14 gives

$$k_p A_p \int d\left(\frac{dT}{dx}\right) = -\frac{I^2\rho}{A_p}\int dx \rightarrow \frac{dT}{dx} = -\frac{I^2\rho}{k_p A_p^2}x + C_1 \qquad 2.15$$

Using the boundary conditions as T_1 at $x = 0$ and T_2 at $x = L$, Eq. 2.15 can be integrated from 0 to L and leads to

$$\int_{T_1}^{T_2} dT = -\frac{I^2\rho}{k_p A_p^2}\int_0^L x + \int_0^L x\, C_1 \rightarrow (T_2 - T_1) \qquad 2.16$$

$$= -\frac{I^2\rho}{2k_p A_p^2}L^2 + C_1 L_p$$

From the above equation, C_1 can be obtained as

$$C_1 = \frac{I^2\rho}{2k_p A_p^2}L_p + \left(\frac{T_2 - T_1}{L_p}\right) \qquad 2.17$$

Substituting Eq.2.17 into Eq.2.15 at $x = 0$ gives

$$\left.\frac{dT}{dx}\right|_{x=0} = -\frac{I^2\rho}{2k_p A_p^2}L_p - \frac{(T_1 - T_2)}{L_p} \qquad 2.18$$

Substituting Eq. 2.18 into Eq. 2.10 yields

$$q_p = \alpha_p T_1 I - \frac{1}{2} I^2 \frac{\rho_p L_p}{A_p} + \frac{k_p A_p}{L_p}(T_1 - T_2) \quad 2.19$$

Eq. 2.19 represents the heat transfer for the p-type, by following the similar way the heat transfer equation for n-type can be derived as

$$q_n = -\alpha_n T_1 I - \frac{1}{2} I^2 \frac{\rho_n L_n}{A_n} + \frac{k_n A_n}{L_n}(T_1 - T_2) \quad 2.20$$

As shown in Eq.2.8, the heat transfer rates of thermoelectric couple equal to

$$\dot{Q}_1 = (\alpha_p - \alpha_n) T_1 I - \frac{1}{2} I^2 \left(\frac{\rho_p L_p}{A_p} + \frac{\rho_n L_n}{A_n} \right) + \left(\frac{k_p A_p}{L_p} + \frac{k_n A_n}{L_n} \right)(T_1 - T_2) \quad 2.21$$

and,

$$\dot{Q}_2 = (\alpha_p - \alpha_n) T_2 I + \frac{1}{2} I^2 \left(\frac{\rho_p L_p}{A_p} + \frac{\rho_n L_n}{A_n} \right) + \left(\frac{k_p A_p}{L_p} + \frac{k_n A_n}{L_n} \right)(T_1 - T_2) \quad 2.22$$

Moreover, the material properties can be added together using the following equations

$$\alpha = \alpha_p - \alpha_n \quad 2.23$$

$$R = \frac{\rho_p L_p}{A_p} + \frac{\rho_n L_n}{A_n} \quad (2.24)$$

$$K = \frac{k_p A_p}{L_p} + \frac{k_n A_n}{L_n} \quad (2.25)$$

where α, R and K are the total Seebeck coefficient: electrical resistance and thermal conductance of the couple, respectively. Simplifying Eqns 2.21and 2.22, using Eqns.2.23 to 2.25 gives

$$\dot{Q}_1 = \alpha T_1 I - \frac{1}{2} I^2 R + K(T_1 - T_2) \quad (2.26)$$

$$\dot{Q}_2 = \alpha T_2 I + \frac{1}{2} I^2 R + K(T_1 - T_2) \quad (2.27)$$

The above two Eqns.2.26 and 2.27 are known as the ideal (standard) equations. The first term $\alpha T_1 I$ is the Peltier/Seebeck effect, which is a reversible process. A higher Peltier/Seebeck effect is needed in order to have a higher cooling or power generation. The second term $\frac{1}{2} I^2 R$ is known as the Joule heating, which is an irreversible process. Finally, the third term $K(T_1 - T_2)$ is the thermal conductance, which is also an irreversible process. The heat flow direction is significant in order to know the type of thermoelectric couple, either a thermoelectric cooler or thermoelectric generator. If the direction of heat flow is same as the direction that

shows in Figure 2.2, then it represents the thermoelectric generator. By reversing the heat flow direction, the thermoelectric cooler can be represented.

2.2.3 Thermoelectric generator [2]

A thermoelectric generator is a power generating device that directly converts thermal energy into electrical energy. When the connected junctions of two dissimilar materials (n-type and p-type) have a temperature difference, an electrical current is generated as shown in Figure 2.3. For a thermoelectric generator, subscript 1 is used for the hot side in equation 2.26 and 2.27 and subscript 2 is used for the cold side.

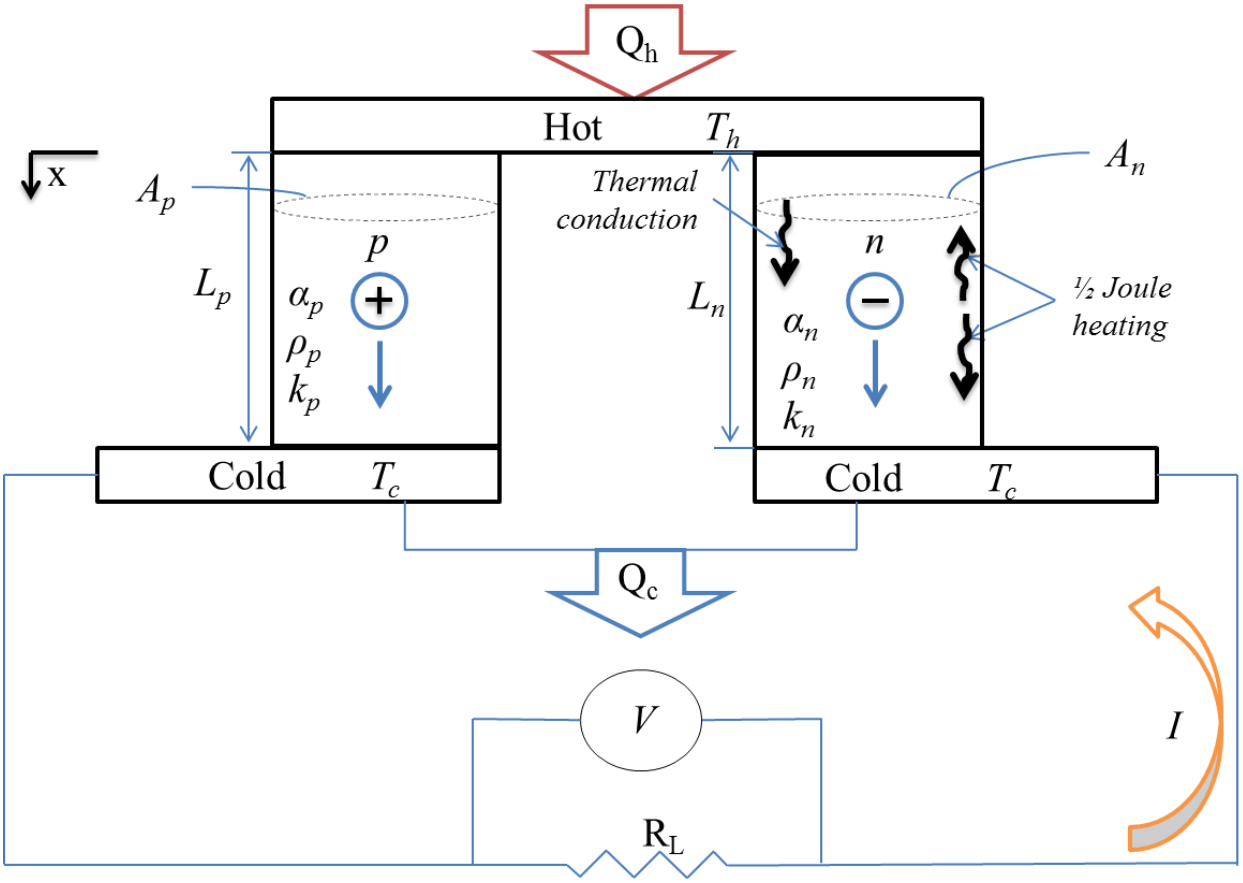

Figure 2.3 An electrical circuit for a unit couple of a thermoelectric generator

$$\dot{Q}_h = \alpha T_h I - \frac{1}{2} I^2 R + K(T_h - T_c) \qquad 2.28$$

$$\dot{Q}_c = \alpha T_c I + \frac{1}{2} I^2 R + K(T_h - T_c) \qquad 2.29$$

By applying the first law of thermodynamics, the electric power $\dot{W}$ generated from the thermocouple is

$$\dot{W} = \dot{Q}_h - \dot{Q}_c \qquad 2.30$$

or

$$\dot{W} = \alpha I(T_h - T_c) - I^2 R \tag{2.31}$$

Also,

$$\dot{W} = I^2 R_L \tag{2.32}$$

where R_L is the load resistance. Moreover, Ohm's Law is defined as

$$V = IR_L = \alpha(T_h - T_c) - IR \tag{2.33}$$

Therefore, current I can be written as

$$I = \frac{\alpha(T_h - T_c)}{R_L + R} \tag{2.34}$$

The thermal efficiency of the thermoelectric generator is defined as the ratio of power output to the heat input

$$\eta_{th} = \frac{\dot{W}}{\dot{Q}_h} \tag{2.35}$$

$$\eta_{th} = \frac{I^2 R_L}{\alpha T_h I - \frac{1}{2} I^2 R + K(T_h - T_c)} \tag{2.36}$$

The output power and thermal efficiency can also be rewritten in terms of R_L/R as follows

$$\dot{W} = \frac{\alpha^2 T_c^2 \left[\left(\frac{T_c}{T_h}\right)^{-1} - 1\right]^2 \left(\frac{R_L}{R}\right)}{R\left(1 + \frac{R_L}{R}\right)^2} \quad 2.37$$

$$\eta_{th} = \frac{\left(1 - \frac{T_c}{T_h}\right)\left(\frac{R_L}{R}\right)}{\left(1 + \frac{R_L}{R}\right) - \frac{1}{2}\left(1 - \frac{T_c}{T_h}\right) + \frac{\left(1 + \frac{R_L}{R}\right)^2 \frac{T_c}{T_h}}{ZT_c}} \quad 2.38$$

For maximum conversion efficiency

$$\frac{d\eta_{th}}{d\left(\frac{R_L}{R}\right)} = 0 \quad \xrightarrow{gives} \quad \frac{R_L}{R} = \sqrt{1 + Z\bar{T}} \quad 2.39$$

where $\bar{T}$ is the average temperature between the hot and cold junction and is equal to

$$\bar{T} = \frac{T_c + T_h}{2} = \frac{1}{2} T_c \left[1 + \left(\frac{T_c}{T_h}\right)^{-1}\right] \quad 2.40$$

As a result, the maximum conversion efficiency, η_{mc}, is

$$\eta_{mc} = \left(1 - \frac{T_c}{T_h}\right) \frac{\sqrt{1 + Z\bar{T}} - 1}{\sqrt{1 + Z\bar{T}} + \frac{T_c}{T_h}} \quad 2.41$$

For maximum power efficiency

$$\frac{d\dot{W}}{d\left(\frac{R_L}{R}\right)} = 0 \quad \xrightarrow{gives} \quad \frac{R_L}{R} = 1 \quad 2.42$$

As a result, the optimum current I_{mp}, maximum power $\dot{W}_{max}$ and maximum power efficiency η_{mp}, are

$$I_{mp} = \frac{\alpha \Delta T}{2R} \tag{2.43}$$

$$\dot{W}_{max} = \frac{\alpha^2 \Delta T^2}{4R} \tag{2.44}$$

$$\eta_{mp} = \frac{\left(1 - \frac{T_c}{T_h}\right)}{2 - \frac{1}{2}\left(1 - \frac{T_c}{T_h}\right) + \frac{4\frac{T_c}{T_h}}{ZT_c}} \tag{2.45}$$

It can be seen from the above equations that the maximum parameters I_{mp}, $\dot{W}_{max}$, and η_{mp} are independent of the load resistance R_L. Therefore, these maximum parameters can be used to generate a generalized graph for TEG as a function of load resistance where output power, voltage, electrical current, and thermal efficiency obtained from equations 2.32,2.33,2.34 and 2.36 respectively, are divided by maximum parameters as shown Figure 2.4. It can be seen from the plot that the maximum output power is when the load resistance is equal to the internal resistance of the thermoelectric couple. Moreover, the thermal efficiency curve follows the same trend of the output power but its maximum value does not appear when the load resistance is equal to the internal resistance.

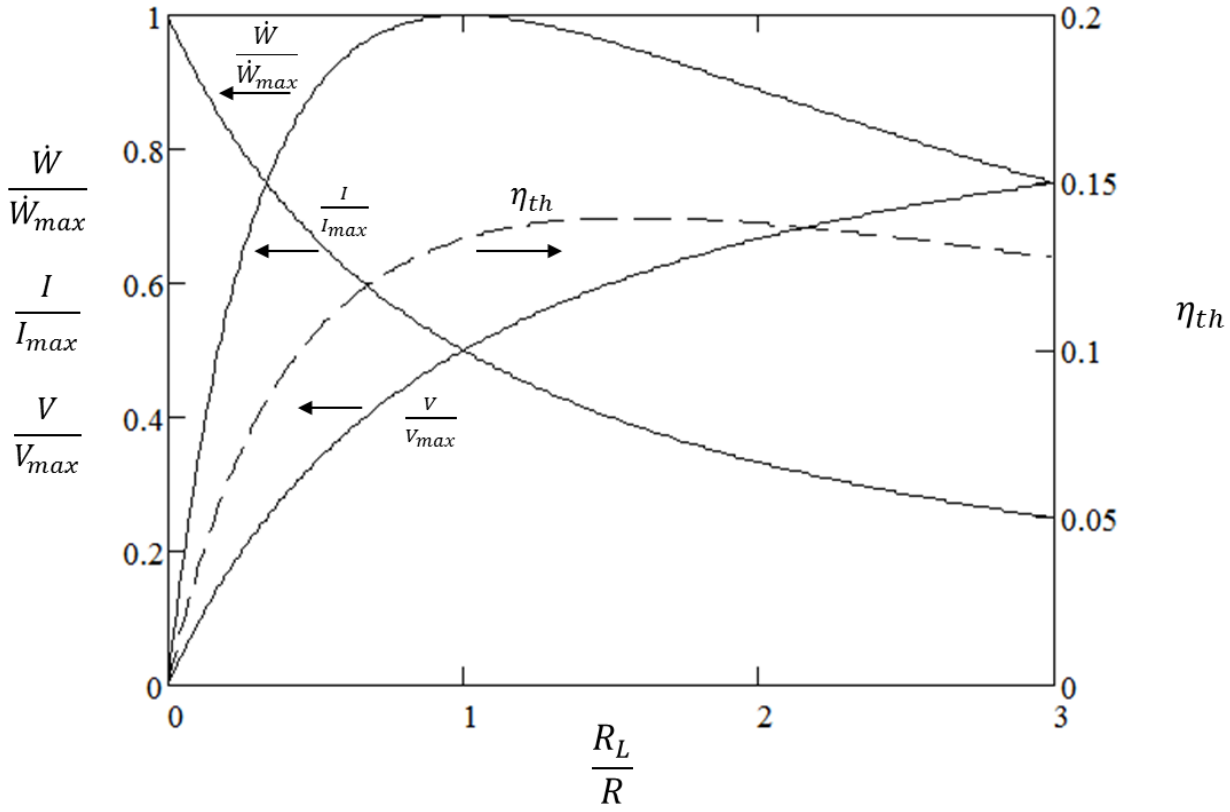

Figure 2.4 Generalized chart of TEG characteristics where ZT=1

This analysis represents the concepts of the thermoelectric generator of one thermocouple where multiple couples are being used in many of the TEG applications. In order to obtain the thermoelectric parameters for multiple couples as shown in Figure 2.5, the unit couple parameters need to be multiplied by the number of couples, n, as follows

$$(\dot{W})_{no} = n\dot{W} \quad 2.46$$

$$(\dot{Q}_h)_{no} = n\dot{Q}_h \quad 2.47$$

$$(R)_{no} = nR \quad 2.48$$

$$(R_L)_{no} = nR_L \quad 2.49$$

$$(V)_{no} = nV \quad 2.50$$

$$(K)_{no} = nK \quad 2.51$$

$$(I)_{no} = I \quad 2.52$$

$$(\eta_{th})_{no} = \frac{(\dot{W})_{no}}{(\dot{Q}_h)_{no}} = \eta_{th} \quad 2.53$$

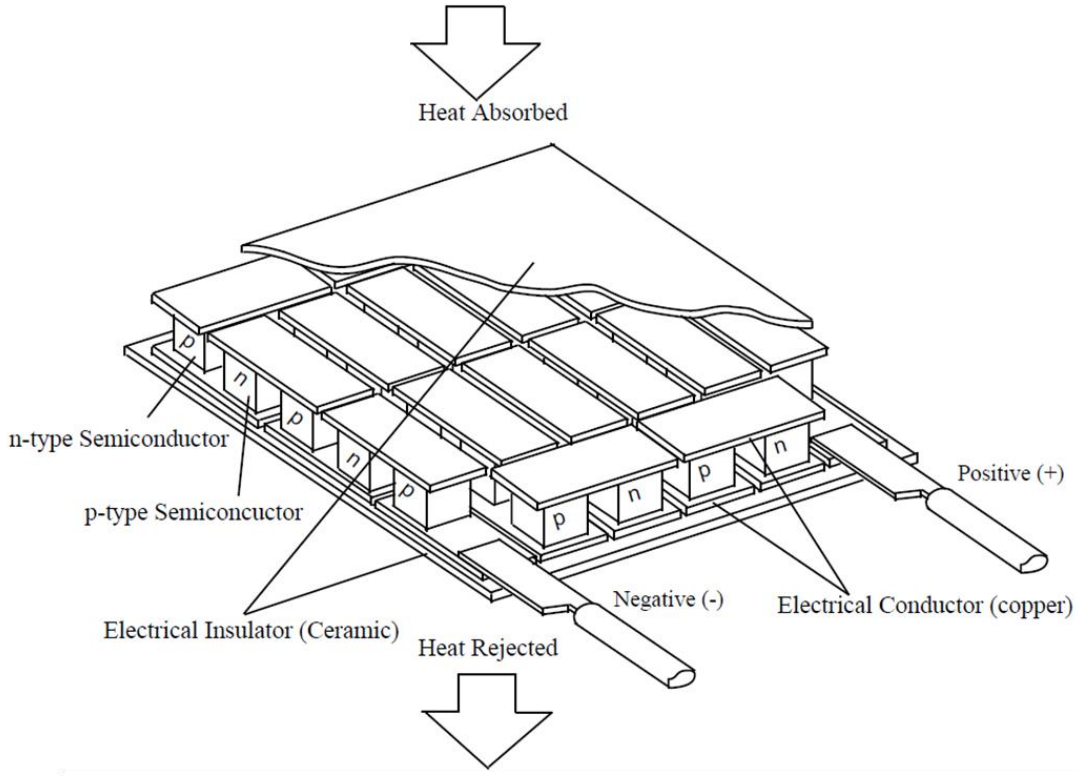

Figure 2.5 A conventional thermoelectric module

2.2.4 Thermoelectric cooler (TEC)

The Seebeck effect is a reversible process. If a current is supplied to a thermoelectric couple, electrons and holes will move through *p* and *n* elements causing heating on one side and cooling on the other as shown in Figure 2.6.

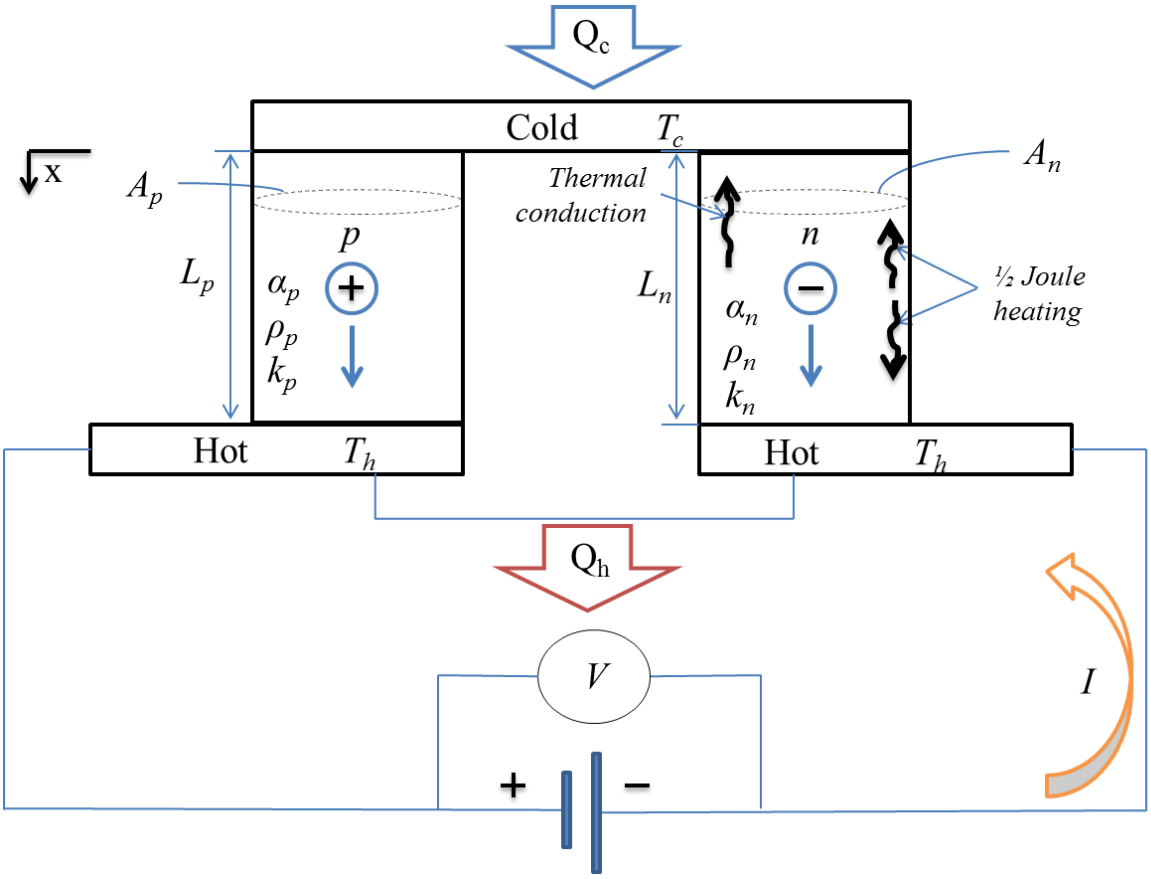

Figure 2.6 A thermoelectric cooler couple

For thermoelectric cooling, subscript 1 is generally used to denote the cold side and subscript 2 is used to denote the hot side which gives [12]

$$\dot{Q}_c = \alpha T_c I - \frac{1}{2} I^2 R + K(T_c - T_h) \qquad 2.54$$

$$\dot{Q}_h = \alpha T_h I + \frac{1}{2} I^2 R + K(T_c - T_h) \qquad 2.55$$

By applying the first law of thermodynamics across the thermocouple, the input power can be defined as

$$\dot{W} = \dot{Q}_h - \dot{Q}_c \qquad 2.56$$

which is also equal to

$$\dot{W} = \alpha I(T_h - T_c) + I^2R \quad 2.57$$

also,

$$\dot{W} = IV \quad 2.58$$

Hence, voltage becomes

$$V = \alpha(T_h - T_c) + IR \quad 2.59$$

The coefficient of performance COP is similar to the thermal efficiency but its value may be greater than 1 and it is defined as the ratio of the cooling power (or heating power) to the input power [12].

$$COP = \frac{\dot{Q}_c}{\dot{W}} \quad 2.60$$

Substituting Equations 2.54 and 2.54 and 2.55 into 2.592.57 gives [13]

$$COP = \frac{\alpha T_c I - \frac{1}{2}I^2R - K\Delta T}{\alpha I\Delta T + I^2R} \quad 2.61$$

where

$$\Delta T = (T_h - T_c) \quad 2.62$$

For maximum cooling power, $\dot{Q}_{c,mp}$, the optimum input current can be found by differentiating Equation 2.542.54 with respect to current and setting it to zero as follows [13]

$$\frac{d\dot{Q}_c}{dI} = \alpha T_c - IR = 0 \xrightarrow{gives} I_{mp} = \frac{\alpha T_c}{R} \quad 2.63$$

The current in Equation 2.63 can also be represented in terms of T_h [13]

$$I_{max} = \frac{\alpha(T_h - \Delta T_{max})}{R} \quad 2.64$$

The maximum temperature difference ΔT_{max} is the maximum possible difference in temperature which always occurs when the cooling power is at zero and the current is maximum. This is obtained by setting $\dot{Q}_c = 0$ in Equation 2.54 substituting both I and T_c by I_{max} and$T_h - \Delta T_{max}$, respectively, and solving forΔT_{max}. The maximum temperature difference is obtained as [13]

$$\Delta T_{max} = \left(T_h + \frac{1}{Z}\right) - \sqrt{\left(T_h + \frac{1}{Z}\right)^2 - T_h^2} \quad 2.65$$

where the figure of merit Z (unit: K^{-1}) is defined as [13]

$$Z = \frac{\alpha^2}{\rho k} = \frac{\alpha^2}{RK} \quad 2.66$$

The maximum cooling power $\dot{Q}_{c,max}$ is the maximum thermal load which occurs at $\Delta T = 0$ and $I = I_{max}$. This can be obtained by substituting both I and T_c in Equation 2.54 by I_{max} and$T_h - \Delta T_{max}$, respectively, and solving for $\dot{Q}_{c,max}$. The maximum cooling power for a thermoelectric module with n thermoelectric couples is [13]

$$\dot{Q}_{c,max} = \frac{n\alpha^2(T_h - \Delta T_{max})}{2R} \quad 2.67$$

The maximum voltage is the DC voltage which delivers the maximum possible temperature difference ΔT_{max} when $I = I_{max}$. The maximum voltage is obtained from Equation 2.59, which is [13]

$$V_{max} = n\alpha T_h \tag{2.68}$$

The maximum COP can be obtained by differentiating Equation 2.61 with respect to current and setting it to zero as follows [13]

$$\frac{d(COP)}{dI} = 0 \xrightarrow{gives} I_{COP} = \frac{\alpha \Delta T}{R\left[(1+Z\bar{T})^{\frac{1}{2}} - 1\right]} \tag{2.69}$$

$$COP_{max} = \frac{T_c}{T_h - T_c} \frac{(1+Z\bar{T})^{\frac{1}{2}} + \frac{T_h}{T_c}}{(1+Z\bar{T})^{\frac{1}{2}} + 1} \tag{2.70}$$

where

$$Z\bar{T} = ZT_h\left(1 - \frac{\Delta T}{2T_h}\right) \tag{2.71}$$

A dimensionless cooling power ($\dot{Q}_c/\dot{Q}_{c,max}$) and COP vs. dimensionless current (I/I_{max}) can be presented graphically as shown in Figure 2.7assuming $ZT_c = 1$. The dimensionless cooling power is obtained from the cooling power found in equation (2.542.54), where the current is the only variable, and from the maximum cooling power equation (2.67) at given thermoelectric material properties and hot side temperature. This generalized plot shows that the cooling power is inversely proportional to the coefficient of performance especially at smaller temperature difference. Moreover, increasing the temperature difference across the junction will decrease the cooling power and the performance of the TEC [13].

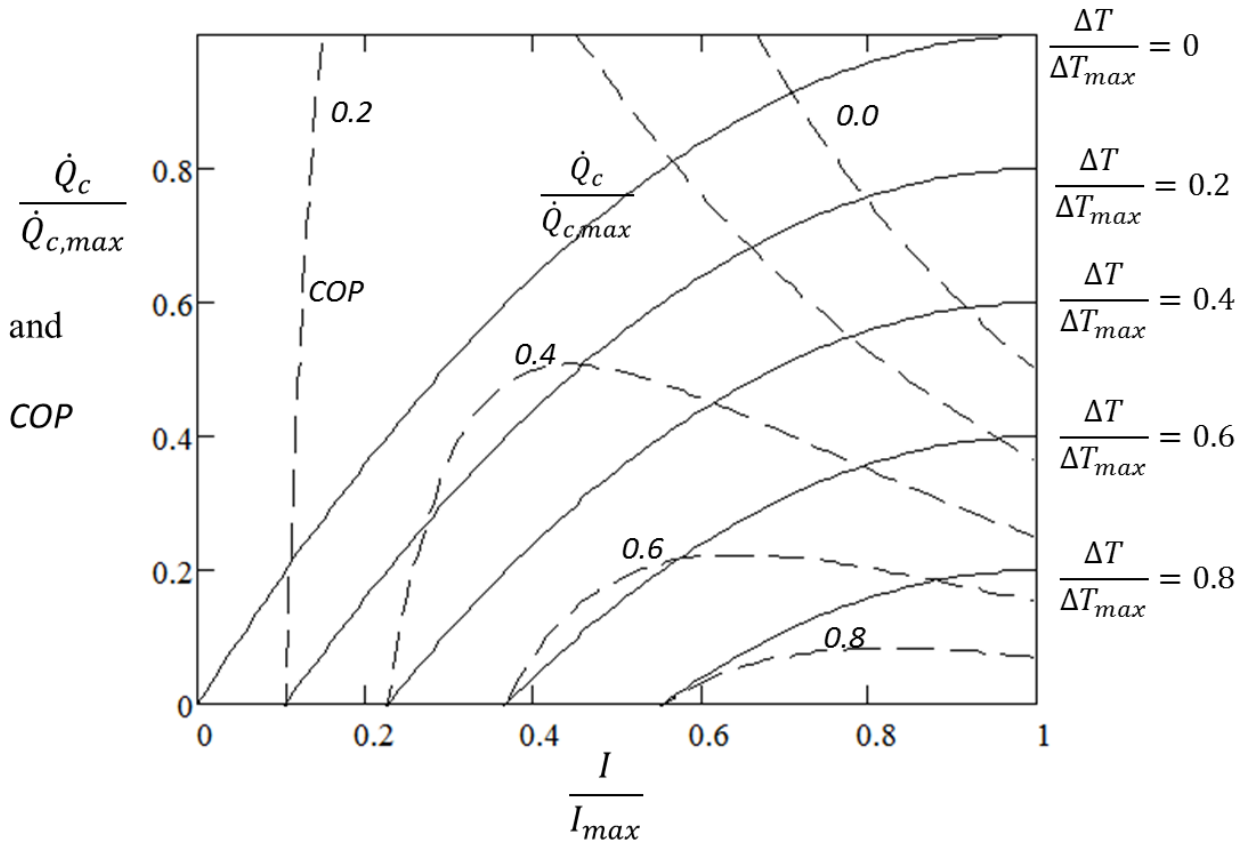

Figure 2.7 Generalized charts for TEC where ZT=1

Similar to the thermoelectric generator, the thermoelectric cooler parameters for multiple couples can be obtained from the unit couple parameters and the number of couples,n as follow [13]

$$\left(\dot{Q}_c\right)_n = n\dot{Q}_c \qquad 2.72$$

$$\left(\dot{Q}_h\right)_n = n\dot{Q}_h \qquad 2.73$$

$$\left(\dot{W}\right)_n = n\dot{W} \qquad 2.74$$

$$(R)_n = nR \qquad 2.75$$

$$(V)_n = nV \qquad 2.76$$

$$(K)_n = nK \tag{2.77}$$

$$(I)_n = I \tag{2.78}$$

$$(COP)_n = \frac{(\dot{Q}_c)_n}{(\dot{W})_n} = COP \tag{2.79}$$

2.2.5 Contact resistances

The thermocouples are usually connected in series by highly conducting metal strips. A number of thermocouples are connected electrically in series and sandwiched between (thermally conducting but electrically insulating) ceramic plates as shown in Figure 2.8. These conductors add electrical and thermal resistances to the system which sometimes increase the discrepancies between the realistic and ideal equation models [14].

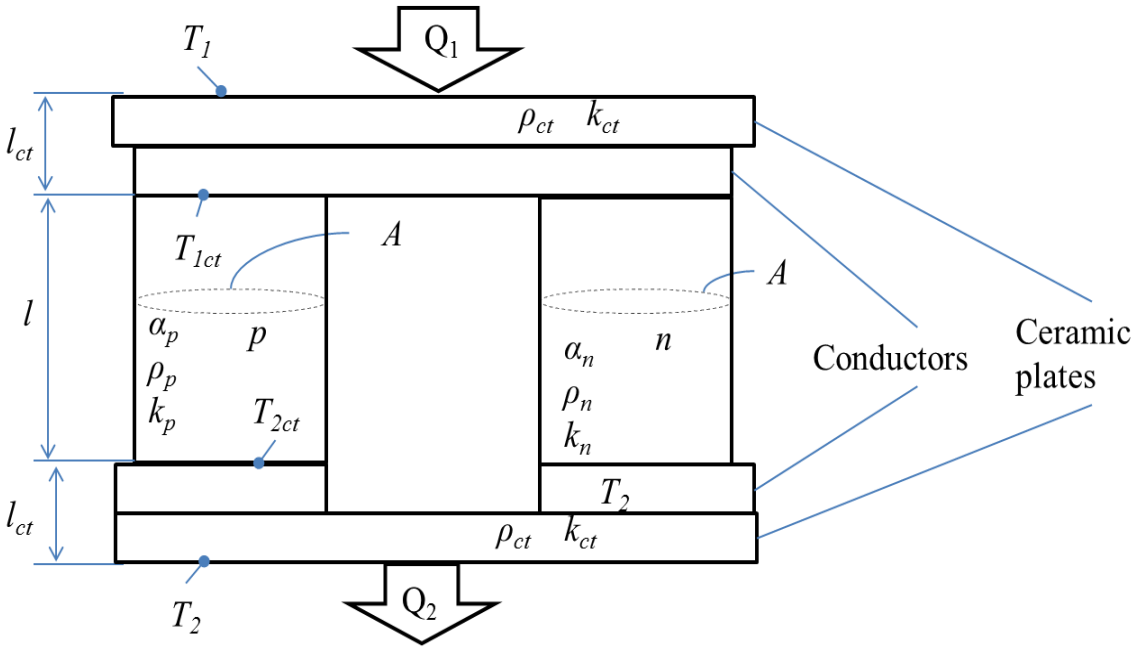

Figure 2.8 A real thermoelectric couple [14]

Consider a single couple thermoelectric cooler where the steady state heat balance can be written as [13]

$$\dot{Q}_1 = \frac{Ak_{ct}}{l_{ct}}(T_1 - T_{1ct}) \tag{2.80}$$

$$\dot{Q}_1 = \alpha I T_{1ct} - \frac{1}{2}I^2R - \frac{Ak}{l}(T_{2ct} - T_{1ct}) \tag{2.81}$$

$$\dot{Q}_2 = \alpha I T_{2ct} + \frac{1}{2}I^2R - \frac{Ak}{l}(T_{2ct} - T_{1ct}) \tag{2.82}$$

$$\dot{Q}_2 = \frac{Ak_{ct}}{l_{ct}}(T_{2ct} - T_2) \tag{2.83}$$

where k_{ct} is the thermal contact conductivity which includes the thermal conductivity of the ceramic plates and thermal contacts and l_{ct} is the thickness of the contact layer. The electrical resistance is composed of the thermocouple and electrical contact resistances as follows [13]

$$R = R_o + R_{ct} = \frac{\rho l}{A} + \frac{\rho_{ct}}{A} = \frac{\rho l}{A}\left(1 + \frac{s}{l}\right) \tag{2.84}$$

where ρ is the electrical resistivity and it is equal to $\rho_n + \rho_p$, ρ_{ct} is the electrical contact resistivity, and s is the ratio between the electrical contact resistivity and electrical resistivity ($s = \rho_{ct}/\rho$). Equations 2.80 to 2.83 are rearranged to have the cooling power per unit area and the coefficient of performance of the TEC module to be [13]

$$\frac{\dot{Q}_1}{nA} = \frac{kT_1}{l}\left[\frac{2Z\bar{T}\xi_{TEC}\left(\frac{T_1}{T_2}+1\right)^{-1}\left(\frac{T_1}{T_2}-1\right)}{\psi\left(1+\frac{s}{l}\right)\left(1-mr\frac{l_c}{l}\right)}\right. \tag{2.85}$$

$$\left. -\frac{Z\bar{T}\left(\frac{T_2}{T_1}+1\right)^{-1}\left(\frac{T_1}{T_2}-1\right)^{2}}{\psi^2\left(1+\frac{s}{l}\right)\left(1-mr\frac{l_c}{l}\right)^{2}} - \frac{\left(\frac{T_1}{T_2}-1\right)}{\left(1-mr\frac{l_c}{l}\right)}\right]$$

$$COP$$

$$= \frac{\xi_{TEC}\left(1-mr\frac{l_c}{l}\right)}{\frac{T_2}{T_1}-1}\frac{\left[\psi - \frac{\frac{T_2}{T_1}-1}{2\xi_{TEC}\left(1-mr\frac{l_c}{l}\right)} - \frac{\psi^2\left(\frac{T_2}{T_1}+1\right)\left(1+\frac{s}{l}\right)}{2Z\bar{T}\xi_{TEC}}\right.}{\psi+1} \tag{2.86}$$

where

$$r = k/k_c \tag{2.87}$$

$$m = 2\left(\frac{Z\bar{T}}{\psi\left(1+\frac{s}{l}\right)}-1\right) \tag{2.88}$$

$$\psi = \sqrt{1+Z\bar{T}}-1 \tag{2.89}$$

$$\xi_{TEC} = \frac{T_{1c}}{T_1}$$

$$= \frac{1+\frac{l_c}{l}\frac{Z\bar{T}\left(1+\frac{T_2}{T_1}\right)^{-1}\left(\frac{T_2}{T_1}-1\right)^{2}}{\psi^2\left(1+\frac{s}{l}\right)\left(1-mr\frac{l_c}{l}\right)^{2}} + r\frac{l_c}{l}\frac{\left(\frac{T_2}{T_1}-1\right)}{\left(1-mr\frac{l_c}{l}\right)}}{1+2r\frac{l_c}{l}\frac{Z\bar{T}\left(1+\frac{T_2}{T_1}\right)^{-1}\left(\frac{T_2}{T_1}-1\right)}{\psi\left(1+\frac{s}{l}\right)\left(1-mr\frac{l_c}{l}\right)}} \tag{2.90}$$

After studying the above equations, it is found that the effect of the contact resistances increases as the length of the element is decreased. Figure 2.9 shows the

cooling power per unit area ($\dot{Q}_1/nA$) presented in Equation 2.85 and COP (Equation 2.86) as a function of length of the element for four different values of r. The figure implies that the greater the contact resistances the smaller the TEC performances. Moreover, decreasing length of the element implies a greater discrepancy from using the ideal equations (when r and s are equal to zero) especially when length of the element is less than $0.1mm$ [13].

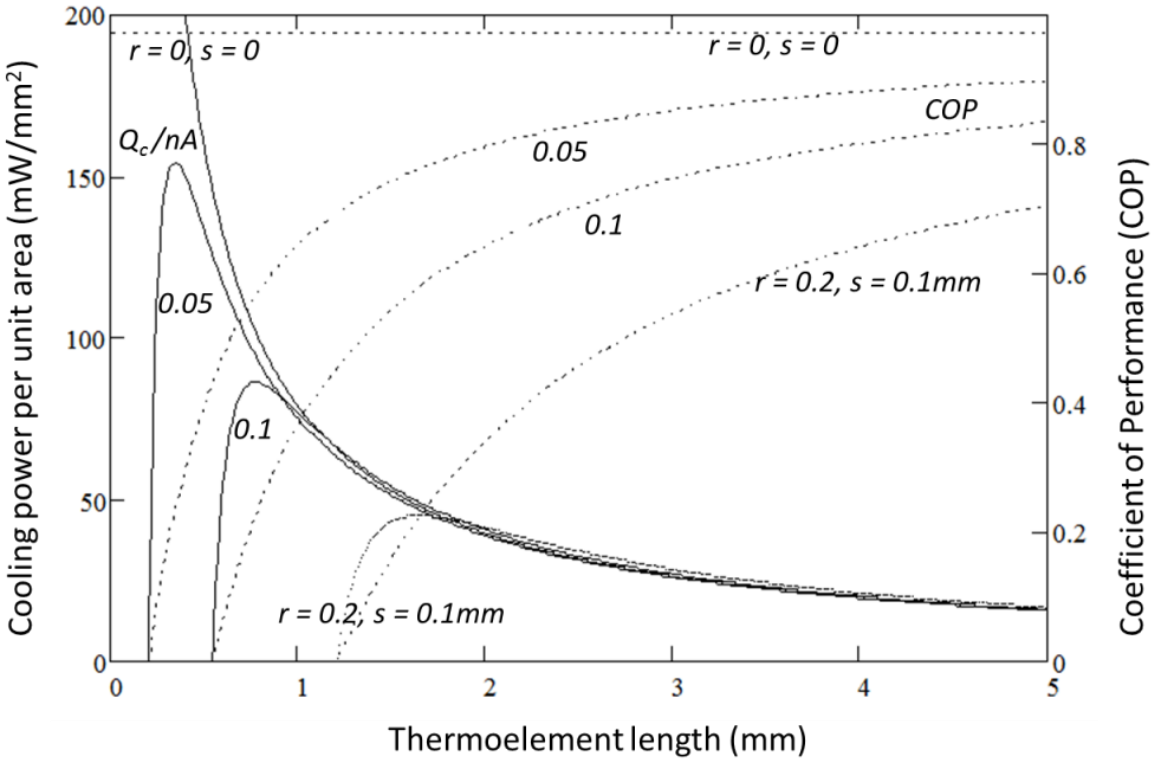

Figure 2.9 Cooling power per unit area and COP as a function of TE length
The above figure is for different values of $\boldsymbol{r}$ and when $\boldsymbol{s = 0.1mm}$, $\boldsymbol{\psi = 0.2}$, $\boldsymbol{k = 1.5W/mK}$, $\boldsymbol{l_c = 0.1mm}$, $\boldsymbol{T_1 = 275K}$, $\boldsymbol{T_2 = 300K}$, and $\boldsymbol{Z = 3 \times 10^{-3}\ K^{-1}}$ [13].

2.3 Thermoelectric System

Typical thermoelectric system is usually attached to heat sinks or heat exchanger devices in order to improve the heat absorption and/or rejection. Once these heat sinks are attached, new equations will be considered along with the ideal equations discussed earlier.

2.3.1 Basic equations

Under steady-state heat transfer, consider the thermoelectric cooler system shown in Figure 2.10. Each heat sink faces a fluid flow at temperature T_∞. Subscript 1 and 2 denote the entities of fluid 1 and 2, respectively. Consider that an electric current is directed in a way that the cooling power $\dot{Q}_1$ enters heat sink 1. We assume that the electrical and thermal contact resistances in the TEC are negligible, the material properties are independent of temperature, the TEC is perfectly insulated, and the p-type and n-type element dimensions are identical. [15]

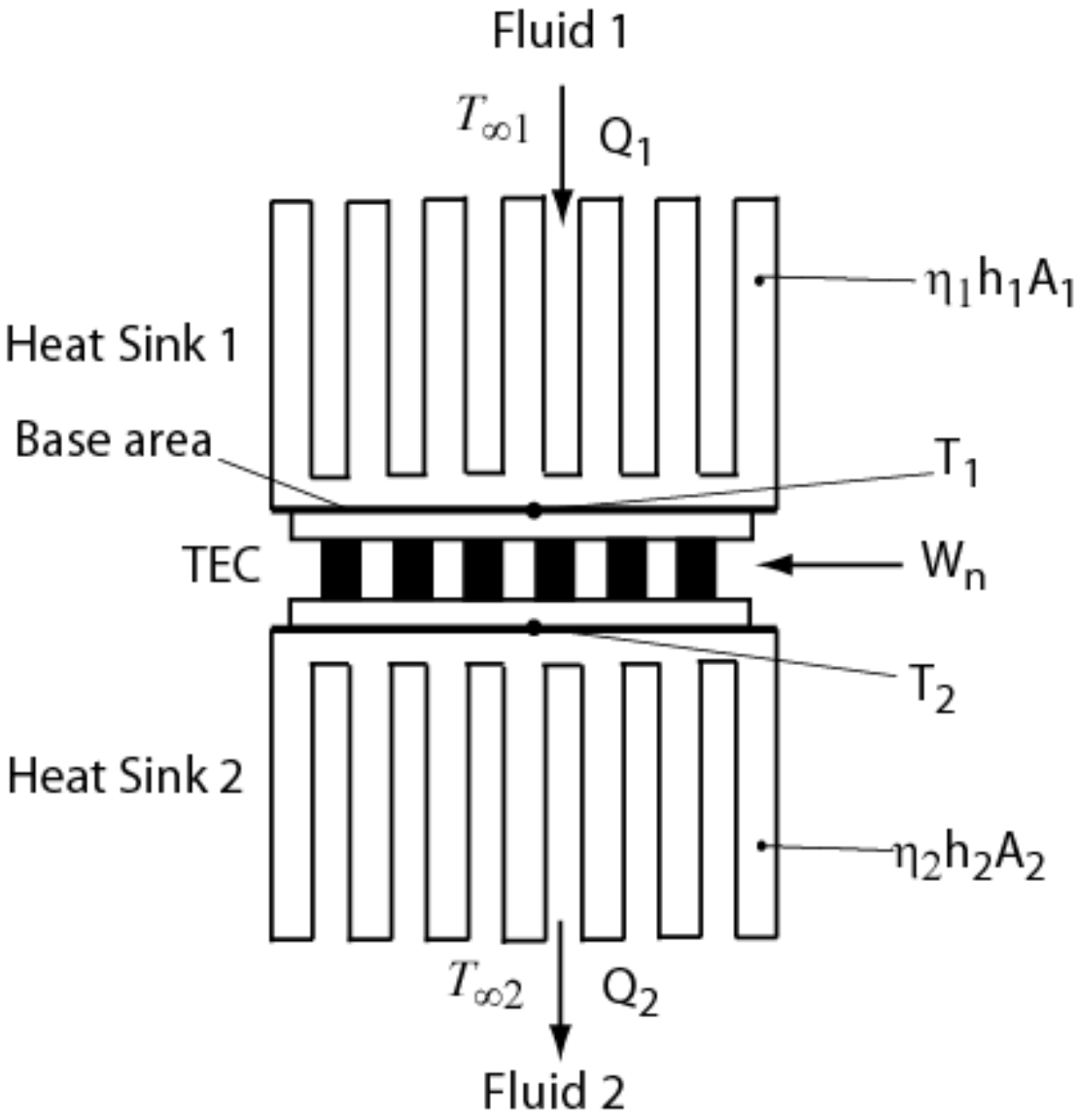

Figure 2.10 Thermoelectric cooler module attached to two heat sinks

The basic equations for the TEC with two heat sinks are given by

$$\dot{Q}_1 = \eta_1 h_1 A_1 (T_{\infty 1} - T_1) \tag{2.91}$$

$$\dot{Q}_1 = n\left[\alpha I T_1 - \frac{1}{2} I^2 R + \frac{A_e k}{L_e}(T_1 - T_2)\right] \tag{2.92}$$

$$\dot{Q}_2 = n\left[\alpha I T_2 + \frac{1}{2} I^2 R + \frac{A_e k}{L_e}(T_1 - T_2)\right] \quad 2.93$$

$$\dot{Q}_2 = \eta_2 h_2 A_2 (T_2 - T_{\infty 2}) \quad 2.94$$

It is noted that the thermal resistances of the heat sinks can be expressed by the reciprocal of the convection conductance (i.e., $\eta_1 h_1 A_1$, where η_1 is the fin efficiency, h_1 is the convection coefficient, and A_1 is the total surface area of the cold heat sink). Also, A_e is the element cross-sectional area, L_e is the element length, and T_1 and T_2 are the heat sinks' 1 and 2 base temperatures respectively which are equal to the thermoelectric module junctions temperatures. [16]

2.4 Heat Sink Design and Optimization

The purpose of attaching a heat sink to the thermoelectric module is to maximize the heat transfer rate from the fins. Therefore, at given dimensions (width, W_f, length, L_f, and profile length, b_f) shown in Figure 2.11, the objective of this section is to optimize the fin thickness, t_f, and fin spacing, z_f of a heat sink in order to minimize the thermal resistance.

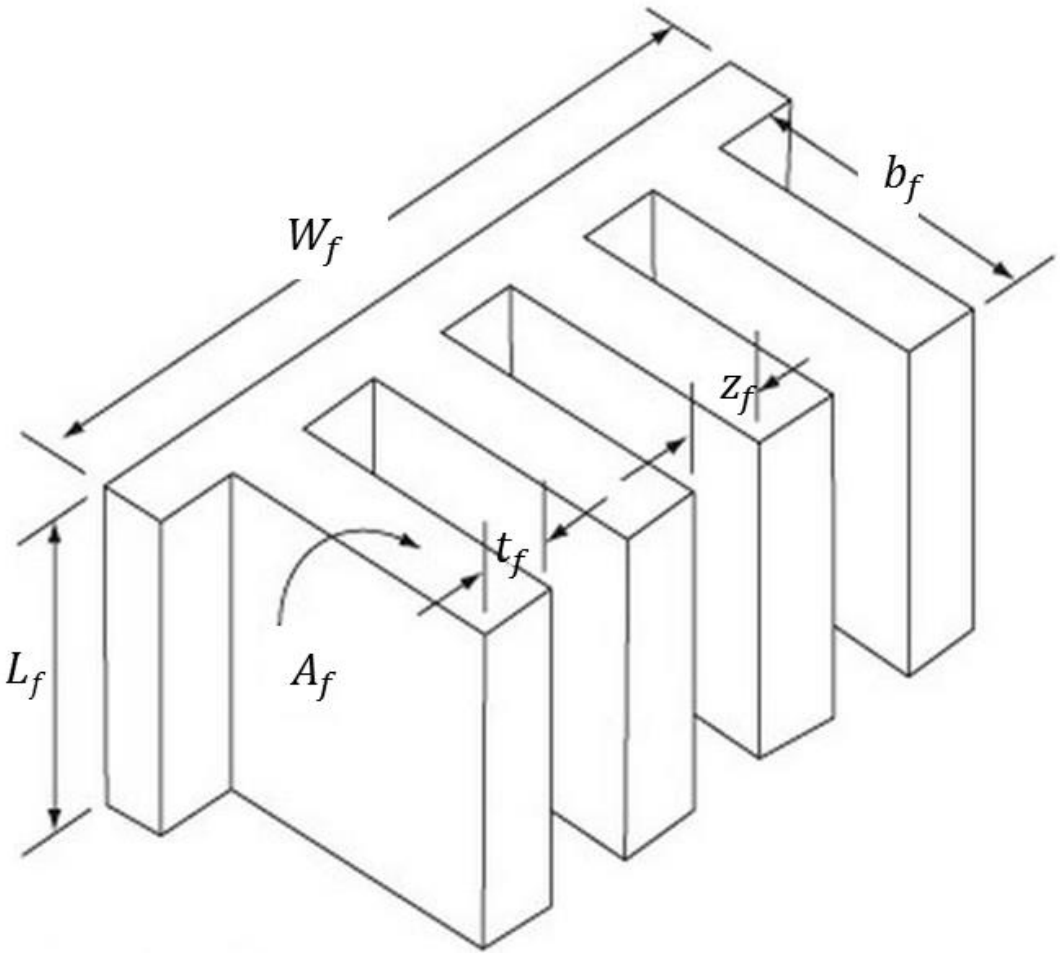

Figure 2.11 Multiple array heat sink [12]

The total fin efficiency is a well-known parameter used to analyze the heat sink thermal resistance and it is defined as follows [13]

$$\eta_f = \frac{\tanh\left[b_f\left(\frac{2h}{k_f t_f}\right)^{1/2}\right]}{b_f\left(\frac{2h}{k_f t_f}\right)^{1/2}} \qquad 2.95$$

where k_f is the thermal conductivity of the fin and h is the heat transfer coefficient of the fluid which can be found from the Nusselt number correlation, Nu, as follow

$$h = \frac{k_{fluid}}{L_f} Nu \tag{2.96}$$

where k_{fluid} is the thermal conductivity of the fluid and L_f is the length of the heat sink that can be replaced by the hydraulic diameter, D_h, for channel flow case. The total heat transfer area of the heat sink is given by

$$A_f = n_f\left[2\left(L_f + t_f\right) + L_f z_{f,opt}\right] \tag{2.97}$$

where n_f is the number of fins. Moreover, it is found that the optimum fin spacing is equal to

$$z_{f,opt} = 3.24 L_f Re_L^{-1/2} Pr^{-1/4} \tag{2.98}$$

where Re_L is the Reynolds number for flow over a plate and Pr is the Prandtl number. After finding the optimum fin spacing for given heat sink parameters, the fin thickness can be optimized to give the maximum heat transfer as follows

$$q_f = \eta_f h A_f (T_\infty - T_b) \tag{2.99}$$

where T_∞ and T_b are the fluid temperatures and the heat sink base temperature respectively [13].

3 Literature Review

3.1 Thermoelectric Cooling (TEC)

The literature showed a number of studies on TEC. The study started off early and in the most recent studies, Terry [17] summarized the phenomena of thermoelectrics, their materials and their applications. Sootsman [18] also briefed thermoelectric concepts in the early ages and the modern developments in thermoelectricity that gives an idea of all the concepts that have already been covered.

A lot of work was done with respect to the element size of a thermoelectric system. Semenyuk.V [19] in an international conference mentioned the working of a miniature thermoelectric device at low temperatures. He also referenced to the improvement in the power density when the ceramic material is changed. The same author in a different work [20] discussed the increase in cooling power of a miniature thermoelectric cooling device.

There has been a good amount of work on the optimization of a thermoelectric model. Zhang [21] in his work discussed about a generalized method of optimizing a thermoelectric cooler. Lee [22] in his work also detailed the readers about a more accurate optimal design method of thermoelectric modules that is used in this work.

3.2 Heat Sink Optimization and its Heat Transfer Coefficient

A typical thermoelectric system consists of a thermoelectric module and two heat exchangers (or heat sinks) attached to both the hot and cold side of the module. It can be seen that the researchers make an effort to combine theoretical

thermoelectric equations and heat sinks equations, and then optimize the geometric parameters of the heat sinks. [23]. Optimization of the heat sinks and heat exchangers are very well established in the literature and Lee [12] summarizes a comprehensive study on the optimization procedures. As for the accuracy of the Nusselt number, analytical correlation can be used but it would be more reliable to have an experimental validation especially for more complicated shapes [24]. Therefore, Teertstra et al. [25] developed an analytical correlation to calculate the Nusselt number based on flow in a parallel plate channel and a combination of developing and fully developed flow. After modifying the Nusselt number correlation to consider the fin effects, they compared the new correlation with experimental values which showed good agreement. Furthermore, Zhimin and Fah [26] used two correlations to calculate the Nusselt number for microchannel heat sinks for both laminar and turbulent flow. The results of the thermal resistances were then validated against other work. These studies of the heat sink optimization and Nusselt number correlation can be adopted on the current work on thermoelectric system.

3.3 Optimum Design of Thermoelectric System

The recent developments in thermoelectrics needs to be addressed in order to investigate their optimum design. Literature shows several methods on how to optimize thermoelectric parameters. Analyzing parameters like the number of thermocouples, the element geometric ratio, and the thermal conductivity, which is defined as the thermal conductance of elements, is a very practical way to study the optimum design of the thermoelectric parameters [27]. The literature also showed

some techniques that can help analyze the optimum design of thermoelectric parameters.

Dimensionless parameters for a thermoelectric cooler system were introduced by Yamanashi [28] in order to optimize thermoelectric parameters. The paper studied the effect of different dimensionless parameters on the TEC performance as a function of dimensionless electrical current. One of the highlights of this paper is to show that the thermal resistance of the hot side of the TEC has a greater impact on the performance than the cold side thermal resistance. Furthermore, this technique gives the ability to obtain the maximum COP when the heat exchanger of the TEC system is provided. Even though Yamanashi technique is not very adoptable due to the difficulties in obtaining the optimum parameters for the cooling power, some researchers applied it and provide useful results. In fact, Xuan [29] was able to use Yamanashi method to optimize the length of the element while Pan et al. [30] studied the optimum design of cooling power for a thermoelectric cooler.

3.4 Objective

After studying all the literature and understanding the basic concepts of thermoelectrics and the concepts that drive a thermoelectric system, it has been found that a practical approach to this problem, though is quiet accurate, is very expensive. A lot of analytical study has been done on the cooling system of a thermoelectric module. In order to prove and validate the theoretical module, experimental work has also been done. In order to understand the physics better, a simulation has been done in order to validate the theoretical model in this work.

The objective of the current work can be defined as *"Design and modeling of a thermoelectric cooling system using theoretical modeling and numerical simulation."*

A lot of analytical work has been done on a thermoelectric cooling system. All the work can be segregated into the following parts.

- Modeling a thermoelectric couple and extending the same to a module. Validating the accuracy of the said model using analytical solution and a numerical simulation.
- Optimizing the module with respect to input parameters and geometry of the module to calculate the maximum output parameters.
- Studying the optimized unit and understanding the same for a system.

The work that has been done in this project includes a simulation using ANSYS 16.0 while validating the theoretical data to prove that the formulae used in theory are self-sufficient to be applied in real life applications. Validation has been done for a single module at leg lengths varying from 0.1mm to 0.5mm with leg area at 0.41mm*0.41mm and a comparison has been done for the same at higher leg lengths varying from 1mm to 1.5mm and leg area at 1mm*1mm.

4 Modeling a Thermoelectric Cooler Module

The modeling of a thermoelectric cooler can be divided into stages. These stages include the design of the module, analytical modeling and a simulation.

4.1 Design

In this section, we will discuss the design of a module starting from a couple design. The inputs and output locations are described and the main parameters that effect the output of a module are explained.

4.1.1 Couple design

A couple as already explained in the previous sections, a couple consists of a p-type semiconductor, n-type semiconductor, copper and a ceramic. The ceramic is an electric insulator while the copper acts as a conductor of electricity. The junction where the copper is soldered to the leg has a material that has an electric contact resistance. This contact resistance plays an important role while calculating the cooling power of a module. This electrical contact resistance especially is very important when the leg length of the element is below 0.5mm. The effect these resistances is explained in detail in the next chapter. The figure below shows the modeling of this design.

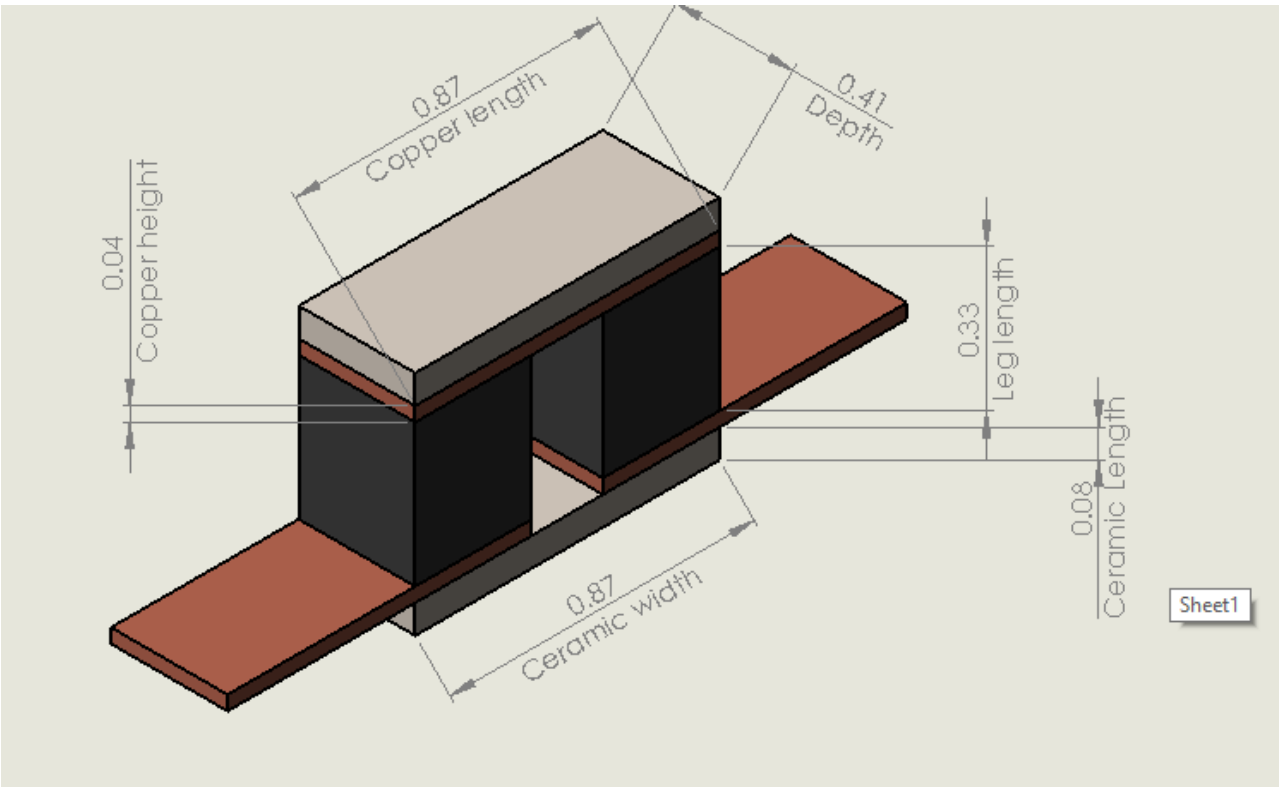

Figure 4.1 Detailed description of a single couple model

The analytical modeling of this design is done as a function of leg length where the leg length is varied in two sets. One of them comprises of miniature leg lengths varying from 0.1mm to 0.5mm. The other comprises of leg lengths varying from 1mm to 1.5mm. The area of the system in the miniature model is taken to be 0.41mm*0.41mm while it's taken to be 1mm*1mm for the macro system.

The length of the copper varies according to the leg dimensions. The height however is set to 0.05mm. The length of the ceramic for a module is set at 0.25mm and the ceramic area for a miniature module is 5.69mm*5.03mm while that for a macro size module increases to 17mm*15mm.

4.1.2 Module design

A module in the current study has 36couples. Like the couple study, the dimensions in the module varies from 0.1mm to 0.5mm in a miniature module while the leg length varies from 1mm to 1.5mm in a macro module. The figure below shows the design of a 36 couple module.

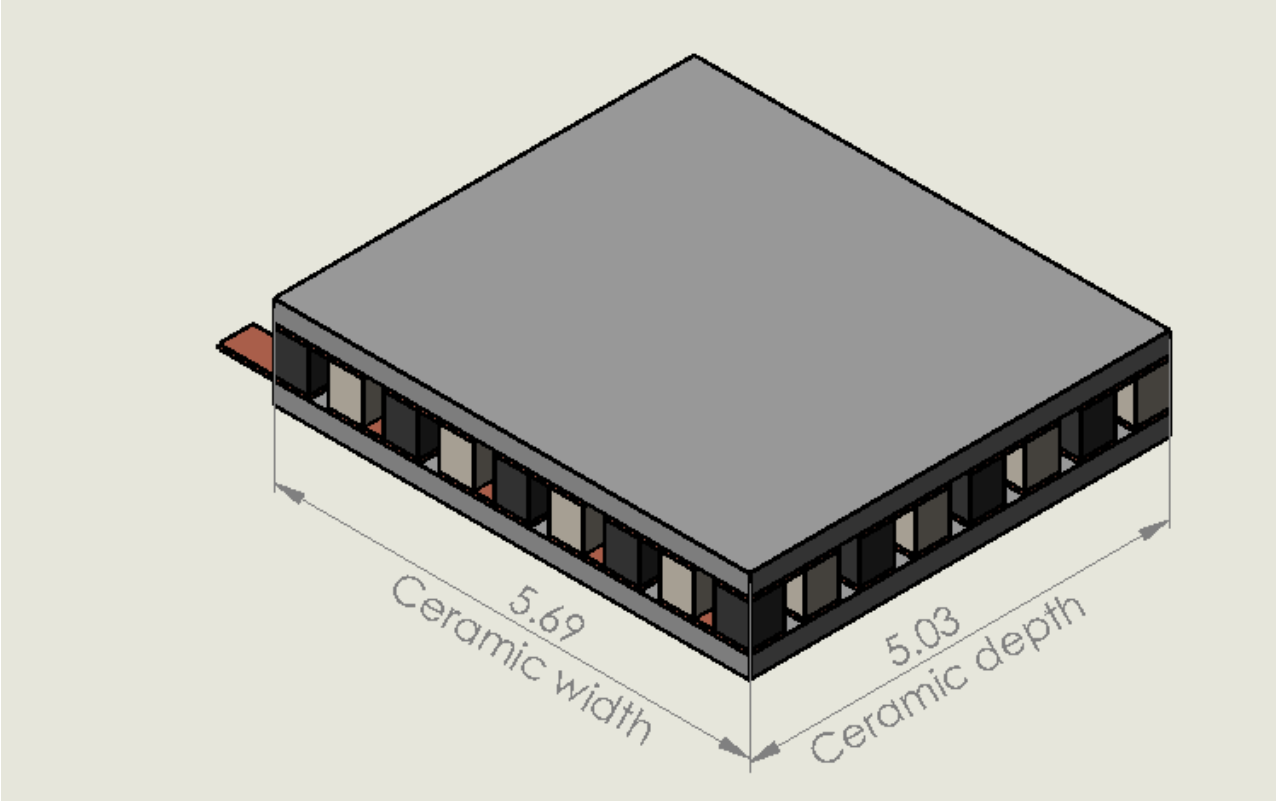

Figure 4.2 36 couple module

4.1.3 Heat Sink design

A heat sink was designed and optimized using the optimization technique developed by Lee [2]. An analysis was done on a system where one thermoelectric module was included that consisted of 127 couples and an optimized heat sink. Heat

sink was fixed on both sides of the thermoelectric module and an air duct was placed in order to input a mass flow rate for air. The input mass flow rate is 3.454g/s. the following figure shows a detailed sketch of the optimized heat sink that was used for this study.

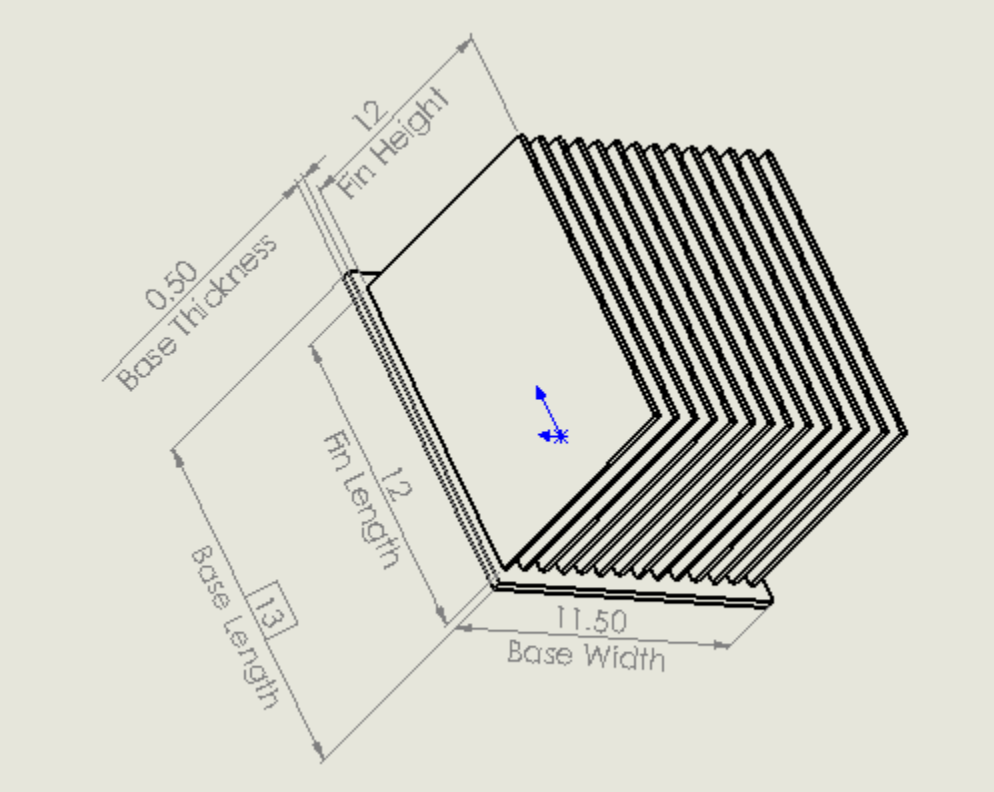

Figure 4.3 Heat sink detailed dimensions

This heat sink is attached to the thermoelectric module where the module is jammed between the heat sinks. The following figure demonstrates this set up.

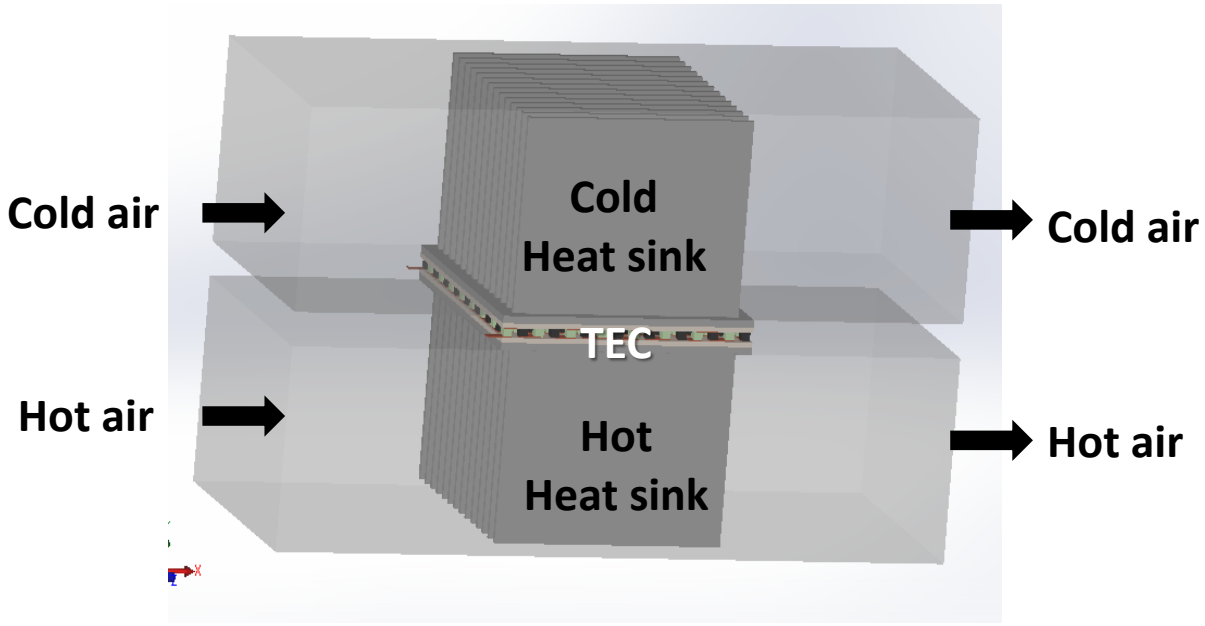

Figure 4.4 Thermoelectric system set up

4.2 MathCad Modeling

Mathcad is a product of MathSoft inc. Mathcad can help us calculate, graph, and communicate technical ideas. It lets us work with mathematical expressions using standard math notation - but with the added ability to recalculate, view, present, and publish with ease, even to the Web.

This software is used to model the setup explained in the previous section. Equations are written in order to calculate the cooling power of the thermoelectric cooler module. While writing the equations, it was observed that the electrical contact resistance and the electrical copper resistance played an important role in determining the output of the said module. Hence, these resistances have been included in all the equations that were written in this work. A result of the effect of these resistances has been discussed in the next chapter. This indicates the amount

of effect these electrical resistances have on the cooling power of a module. Following figure shows the interface of MathCad and the equations that have been used in the analysis.

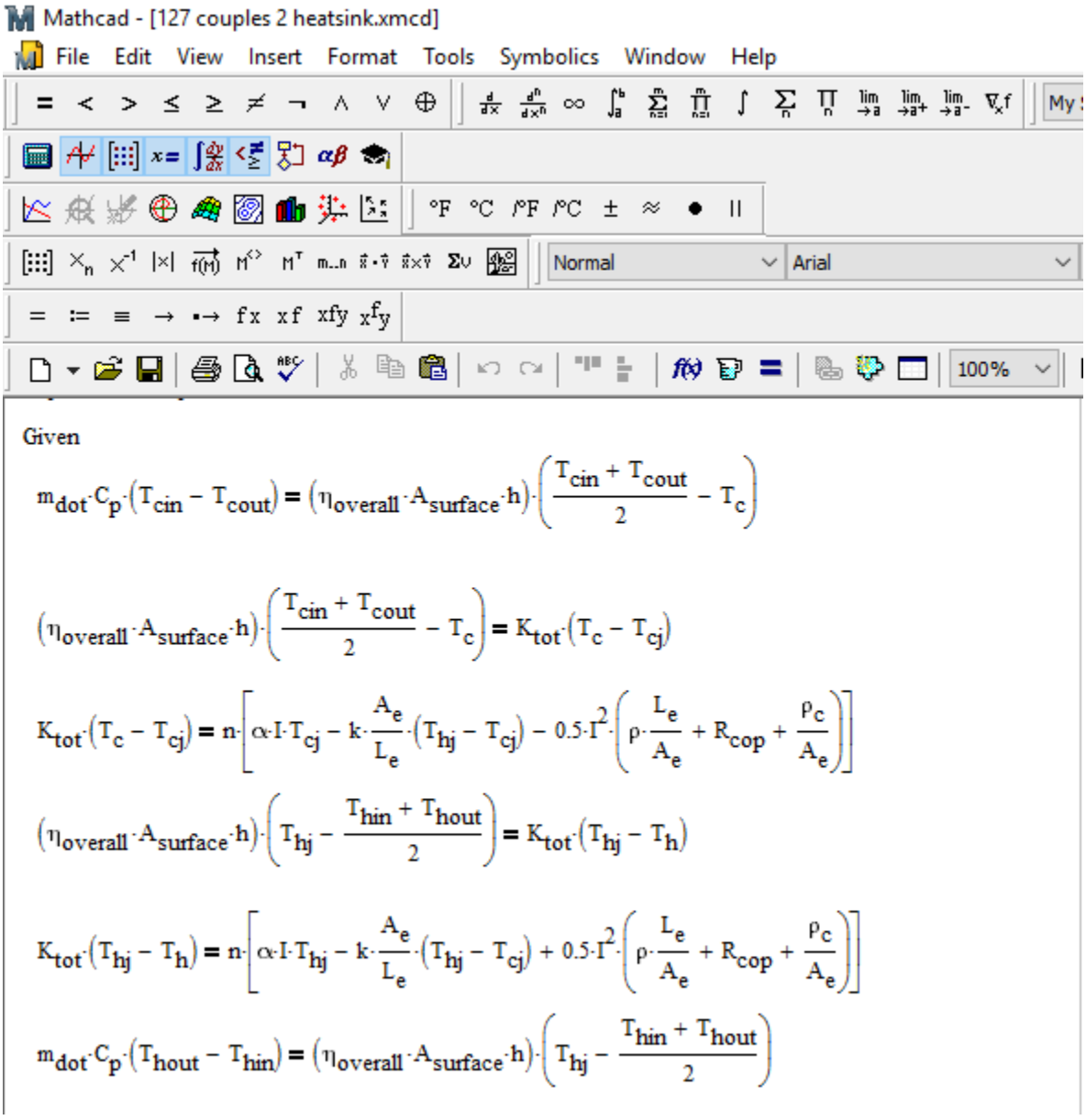

Figure 4.5 MathCad user interface and equations used during the analysis

4.3 ANSYS Simulation

ANSYS is a software that is used for simulation of mechanical components. It has been used in the industry for a long time. It is a Multiphysics software that is able to integrate two or more physics into one to study the behavior of the component with respect to both the physics. The study that is based in this project is an integration between the Computational Fluid Dynamics (CFD) and the thermal electric module. This integration helps in linking both of these together to solve for the cooling effect of the module in question by pulling out results from one another. The following figure shows the setup as an integration between CFD and thermal electric module in ANSYS to numerically solve for the solution of the module given the inputs and boundary conditions.

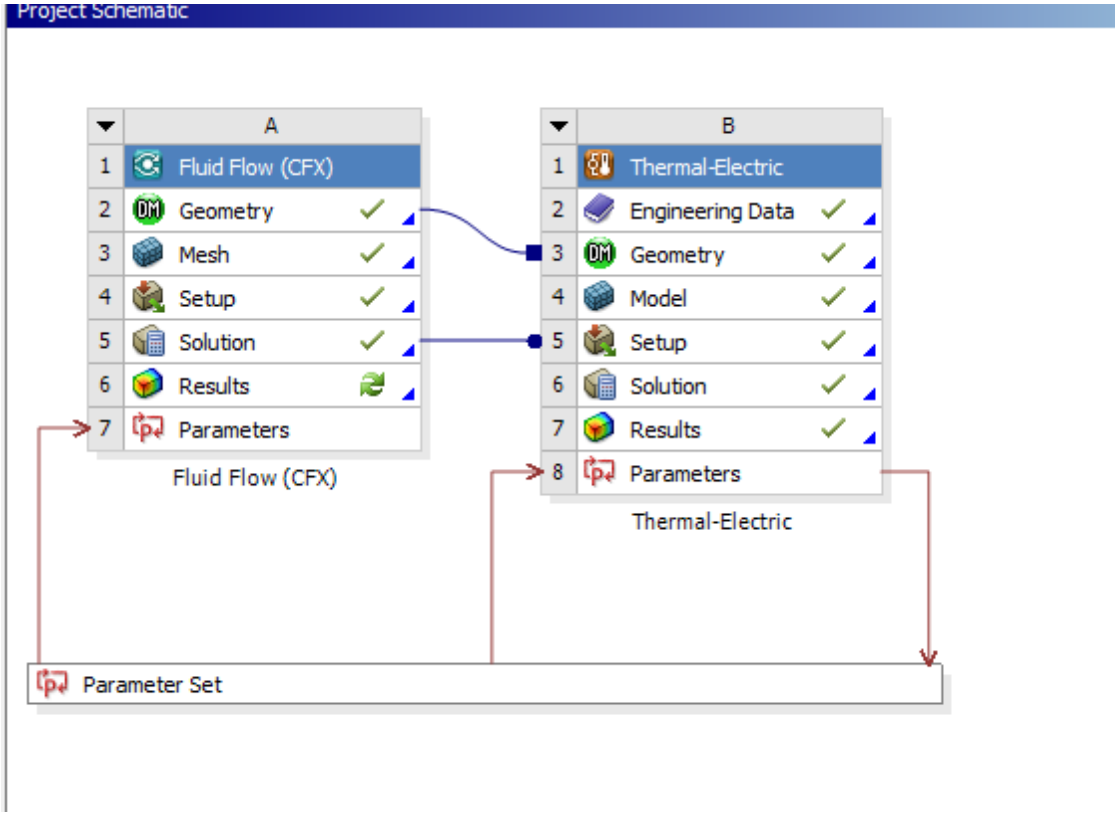

Figure 4.6 ANSYS interface

In the figure shown above, the leg length of the thermoelectric module has been parameterized so that the variation of the cooling power can be obtained at different leg lengths without having to change the leg length manually for each simulation.

5 Results and Discussions

All information in this chapter is with respect to the methodologies explained in Ref. [31], [32], [13], and [33] with the author's contribution. In this chapter, validation of existing thermoelectric module is done to prove the authenticity of the ideal equations. A comparison is done between the analytical modeling and ANSYS simulation of the modules under various conditions. Initially, a comparison is done between the results of MathCad and ANSYS when contact resistance is included and excluded and to understand its importance at low leg lengths. Once its importance has been established, the focus is then shifted to electrical contact resistance of copper. Then, a validation is done of the thermoelectric ideal equations using MathCad and ANSYS. The discussion is then extended to the module when heat sinks are introduced. All discussions are made at low leg lengths (0.1mm-0.5mm), also called miniature devices and bigger leg lengths (1mm-1.5mm) also called macro devices or rather commercial modules. Following dimensions and material properties have been used for all the results.

Table 1 Module specifications used in the study

Geometry	Value	Units
P type-miniature		
Thermal Cross Section Area	0.41mm*0.41mm	mm^2
Length	0.1mm-0.5mm	mm
P type-macro		
Thermal Cross Section Area	1mm*1mm	mm^2
Length	1mm-1.5mm	mm
Seebeck Coefficient (α_p)	210	μV/K
Thermal Conductivity (k_p)	1.6	W/m*K
Electrical Resistivity (ρ_p)	$1*10^5$	Ω*m
N type-miniature		
Thermal Cross Section Area	0.41mm*0.41mm	mm^2
Length	0.1mm-0.5mm	mm
N type-macro		
Thermal Cross Section Area	1mm*1mm	mm^2
Length	1mm-1.5mm	mm
Seebeck Coefficient (α_p)	210	μV/K
Thermal Conductivity (k_p)	1.6	W/m*K
Electrical Resistivity (ρ_p)	$1*10^5$	Ω*m

Table 1 - continued

Copper Conductor-miniature		
Electrical Cross Section Area	0.05mm*0.41	mm^2
Electrical Length	0.87	mm
Copper Conductor-macro		
Electrical Cross Section Area	0.1mm*1mm	mm^2
Electrical Length	2.90	mm
Thermal Conductivity (k_{cop})	401	W/m*k
Electrical Resistivity (ρ_{cop})	1.67*10^-5	Ω*mm
Ceramic Insulation-miniature		
Thermal Cross Section Area	5.06*5.34	mm^2
Length	0.05	mm
Ceramic Insulation-macro		
Thermal Cross Section Area	11.50*13	mm^2
Length	0.1	mm
Thermal Conductivity (k_{cer})	27	W/m*K
Current	2	A
Contact Material		
Sheet Electrical Resistivity (ρ_c) (solder material)	1.68*10^-6	Ω*cm^2

5.1 Contact Resistance

Contact resistance is a parameter in studying the behavior of thermoelectric materials that defines the total output of a given module. In the following discussion, we understand the importance of contact resistance as a function of leg length of the module.

The following graphs show the change in power output when contact resistance is included at a constant input power. The current input in this set up is constant. We can see that there is a maximum power at a certain leg length.

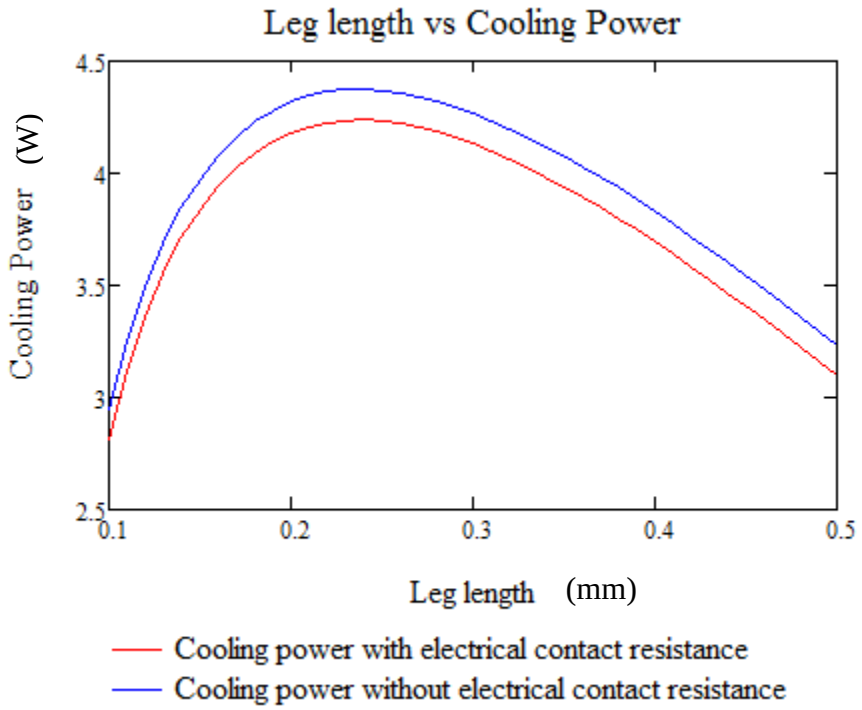

Figure 5.1 The cooling power of a miniature module as a function of leg length

The above figure is at a constant current with leg length varying from 0.1mm to 0.5mm and current 2A.

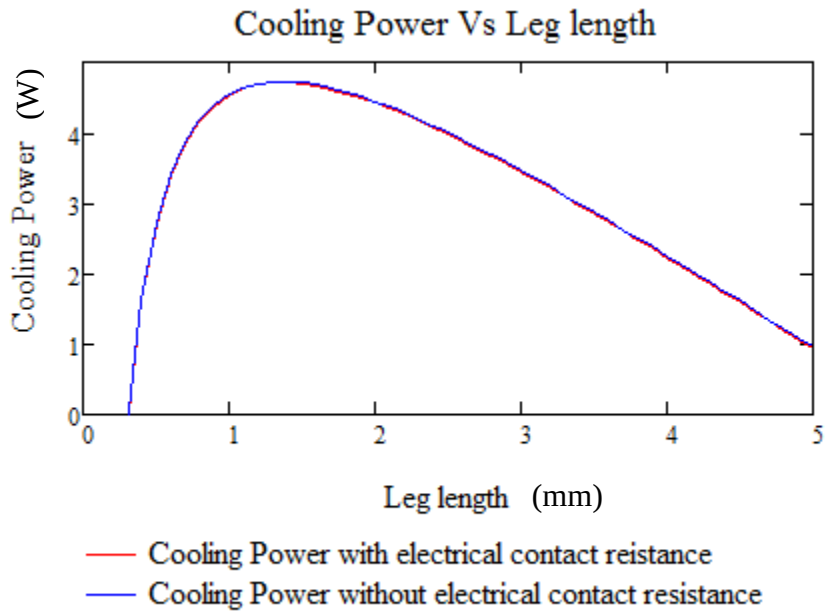

Figure 5.2 The cooling power of a macro module as a function of leg length

The above figure is at constant current with leg length varying from 0.5mm to 5mm and current 2A.

The figures above show the relation between cooling power and leg length. They show the effect of electrical contact resistance at various leg lengths. It can be seen that at lower leg lengths, the effect is more evident. The discrepancy between the calculated thermoelectric cooling effects is higher when compared to the effect at

higher leg lengths. This is mainly due to the fact that at lower leg lengths, the value of the electrical contact resistance is in the same order of magnitude when compared to the electrical resistance of the element. While the value is almost negligible at higher leg lengths.

5.1.1 Optimized comparison

In order to find out the performance of a module in a more experimental point of view, the input current was optimized at each leg length. In the following figure, a comparison is made with respect MathCad calculations and ANSYS simulation.

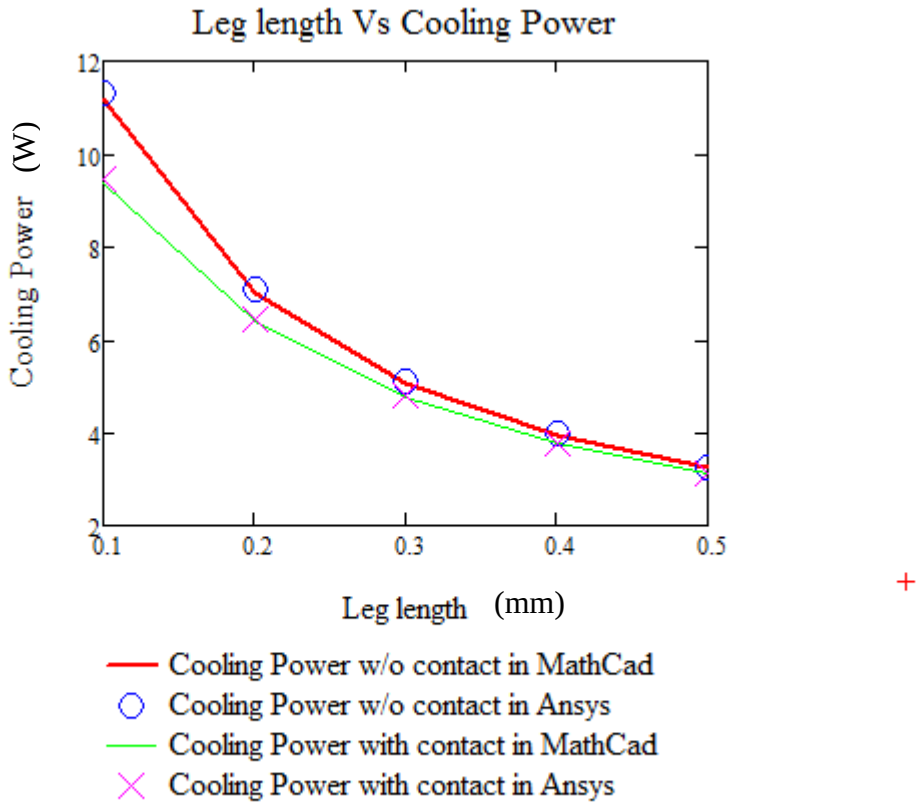

Figure 5.3 Cooling power with and without electrical contact resistance

The figure above is at optimum current for lower leg lengths with current of 2A and hot side temperature 310K and cold side temperature 288K.

The figure above shows the variation of cooling power with varying leg lengths. From this figure, we can say that contact resistance plays an important role at low leg lengths and there is a significant difference in the power output at around 0.2mm leg length. And as the leg length increase to 0.5mm, the impact of contact resistance is also significantly reduced. The current input for each of these leg lengths is

optimized and the plot shows the maximum power obtained at each of these leg lengths.

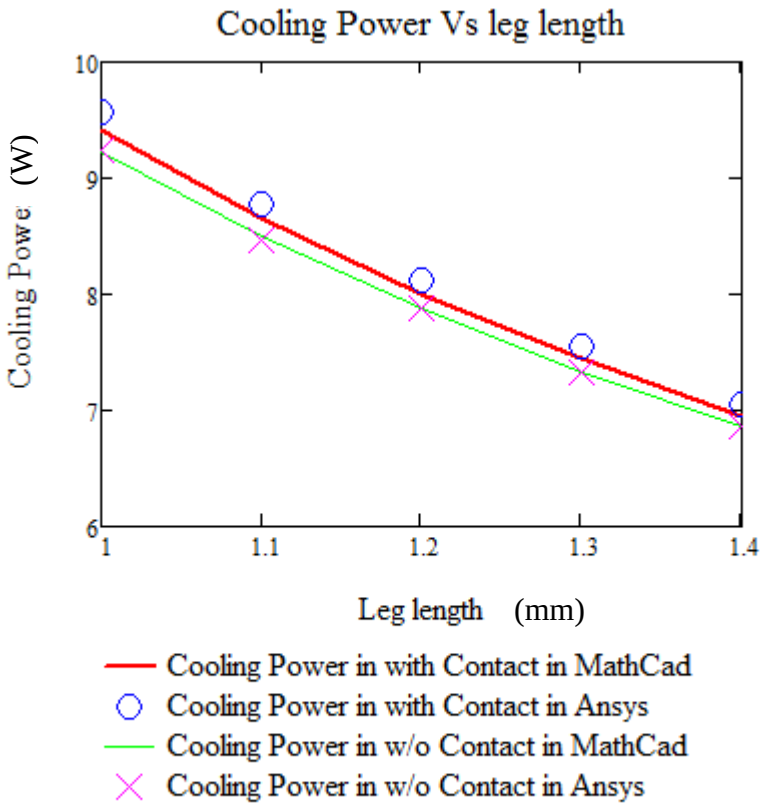

Figure 5.4 Cooling power with and without electrical contact resistance

The above figure is at optimum current for higher leg lengths with current of 2A and hot side temperature 310K and cold side temperature 288K.

It can be seen from this plot that the impact of contact resistance is very less and can as well be neglected at leg lengths about 1mm. The difference in the cooling

power is less than 0.5W. We can also see in the two plots here that the ideal equations are in good agreement with ANSYS simulation. The ANSYS simulation is very close to a real life experiment and hence can be considered a predictable measurement.

5.2 Copper Resistance

We know that copper is an electric conductor. This material also has an electric resistance and though the value is very low, it has a significant importance under certain conditions. The plots below show the difference in cooling power when the resistance of copper is not included. ANSYS considers a default value of electrical resistance of copper while MathCad requires manual input.

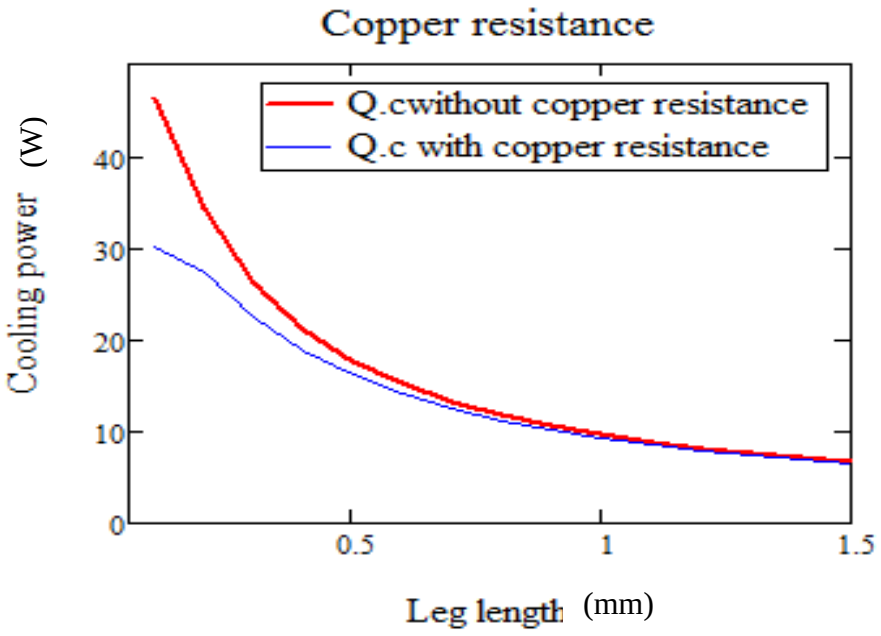

Figure 5.5 Impact of electrical copper resistance

In the figure above, when we look at lower leg lengths, i.e. leg lengths lesser than 0.3mm, the deviation from the actual cooling power is very high. The difference is almost 20W. This means that the mathematical definition given to copper resistance is extremely important and it has to be included. Without the copper resistance, the cooling power obtained mathematically is over predicted. One of the main reasons for this effect for copper electrical resistance is its geometry. A thickness of 0.1mm is considered and at leg lengths of 0.1mm in the thermoelectric module, the copper electrical resistance starts dominating the effects of thermoelectrics. This impacts the cooling power majorly and hence the overall cooling power reduces at this geometry. If the geometry of copper is considerably reduced with a reduction in the leg length, its impact will also significantly reduce hence giving a considerable cooling power.

Since the impact of electrical contact resistance and electrical copper resistance has been established, we can conclude that its effects are rather significant and hence these resistances have been included in all our discussions irrespective of the leg lengths.

5.3 Overall Impact of Electrical Contact Resistance and Electrical Copper Resistance

The impacts of these electrical resistances have been discussed in detail in the previous sections. In this section, we will discuss about the overall impact of

electrical copper and contact resistances together. Their impact as a function of leg length will be discussed in this section.

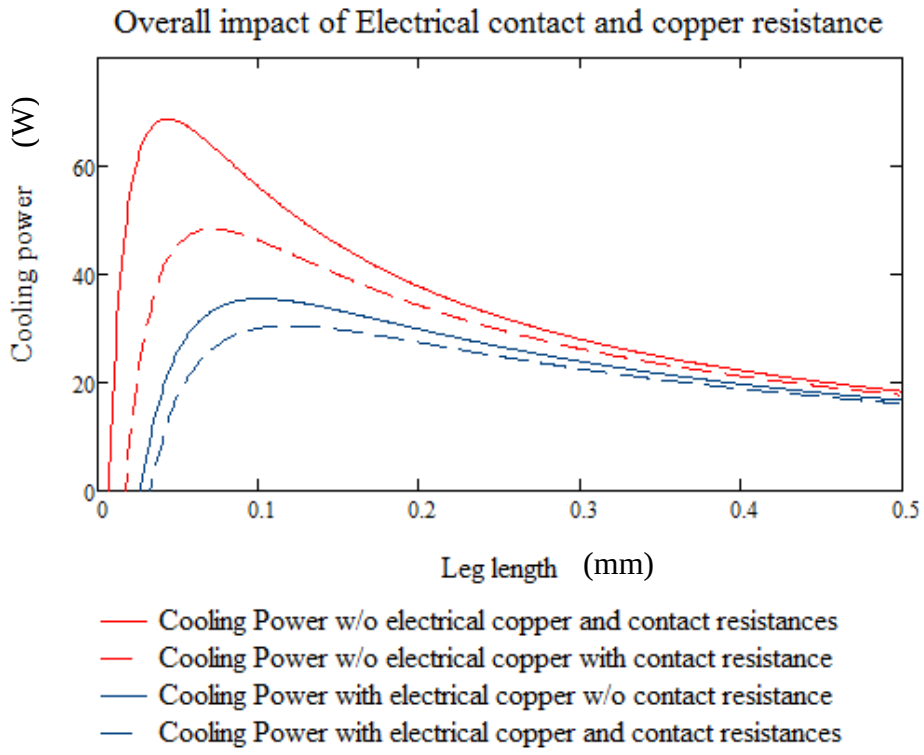

Figure 5.6 Overall impact of electrical copper and electrical contact resistance

The above figure is at current 2A and hot side temperature 310K and cold side temperature 288K.

In the figure above, the red colored solid lines show the cooling power at varying leg lengths when copper electrical resistance is neglected in theoretical calculations while the blue line show the value of cooling power when copper electrical resistance is included. We can see that under the same conditions, the difference in

the calculated cooling power is very significant when electrical resistances of copper and contact are included. Especially at low leg lengths, the difference in the power is almost 30W. This power difference corresponds to a percentage error of almost 53%. Such high errors are caused especially when the leg length is around 0.2mm. At these values of leg lengths, the power predicted using analytical modeling is over predicted. This is a huge difference and hence it can be concluded that both electrical contact resistance and copper electrical resistance play an important role in calculating the cooling power of a given module. As mentioned in the previous section, since it has been established that the effect is higher in few cases while it is not much in others, these resistances have been included in all the equations for calculating the cooling power of the module in question.

5.4 Comparison of Real Values to Ideal Equations

Ideal equations are theoretical equations that are modeled in order to predict the performance of a thermoelectric module under ideal conditions. These equations neglect all kinds of contact resistances. These resistances include the electrical contact resistance, the copper electrical resistance and the thermal contact resistance. In this section, we will discuss about the difference in the prediction of performance theoretical calculations are made using ideal equations and real equations.

The figure below shows the performance prediction of a thermoelectric cooler when calculated using ideal equations and real equations. In the curve obtained by the ideal equations, we can see that, as leg length reduces, there is an exponential

increase in the power output. This situation however, is not practical. There is an optimum value of leg length in the real case beyond which the cooling power is reduced due to the dominance of contact resistances. Hence, at these leg lengths, the cooling power is realistically defined by including the thermal contact resistances, electrical contact resistances and the copper electrical resistances.

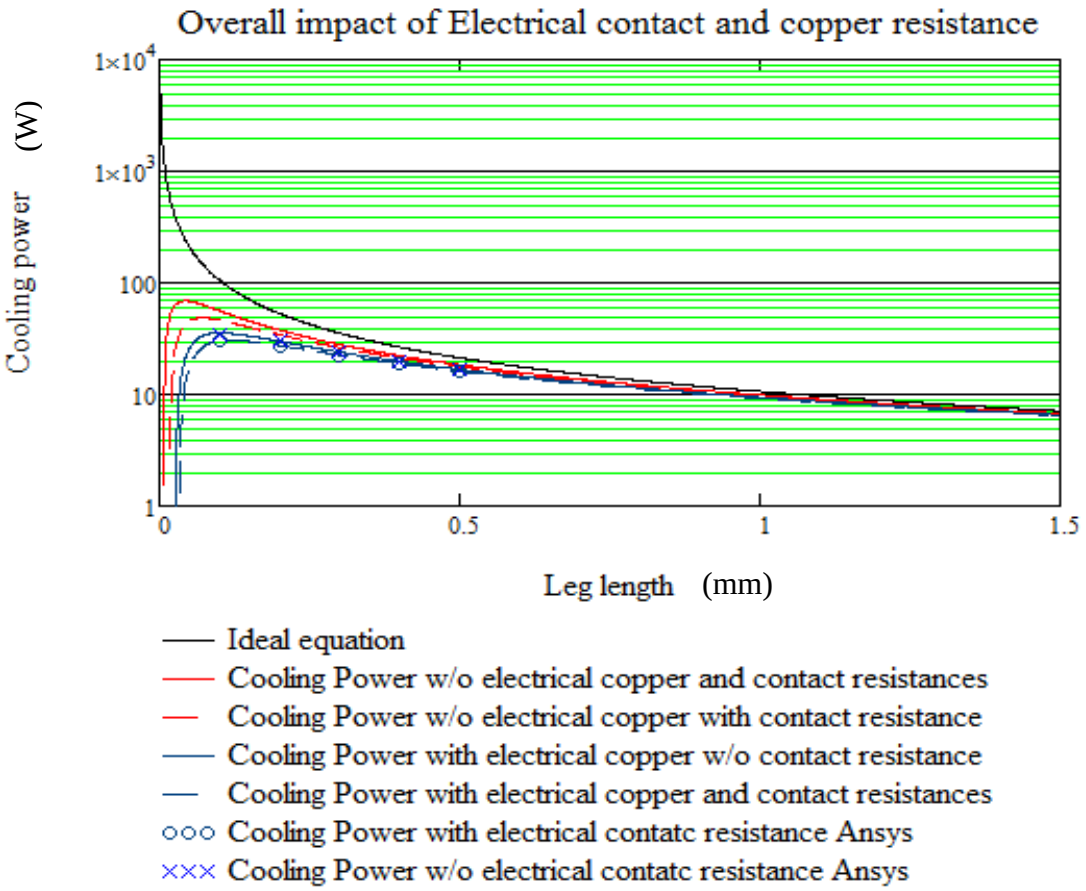

Figure 5.7 Prediction of cooling power using ideal equations vs real equations

5.5 Effect of Heat Sink

5.5.1 Set up and result

In order to study the effect of heat sink in a TE system, the developed Mathcad equations were verified with an ANSYS setup that integrated fluent flow with thermoelectric module. Using Lee's [2] optimum design technique, an optimum heat sink was designed along with thermoelectric module. The module consisted of 127 couples. The leg length used in this setup is 1mm. the thickness of copper is 0.1mm and the length of copper is 2.90mm. The ceramic designed for this set up is 30mm*30mm and the thickness of ceramic is 0.50mm. An air duct is designed in order to analyze forced convection, with a given velocity and a given mass flow rate.

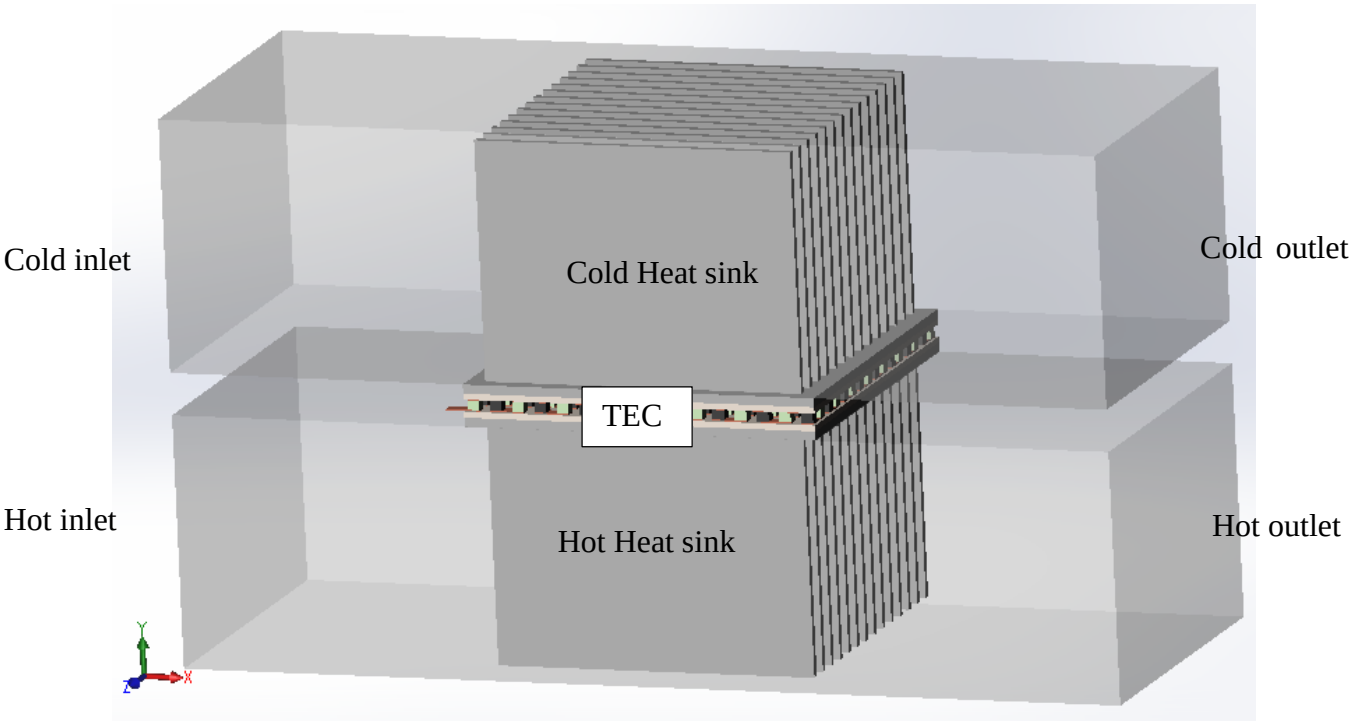

Figure 5.8 Thermoelectric system setup for fluent analysis

As discussed in earlier sections, ANSYS simulation for this setup needs an integration of CFD model and thermoelectric model.

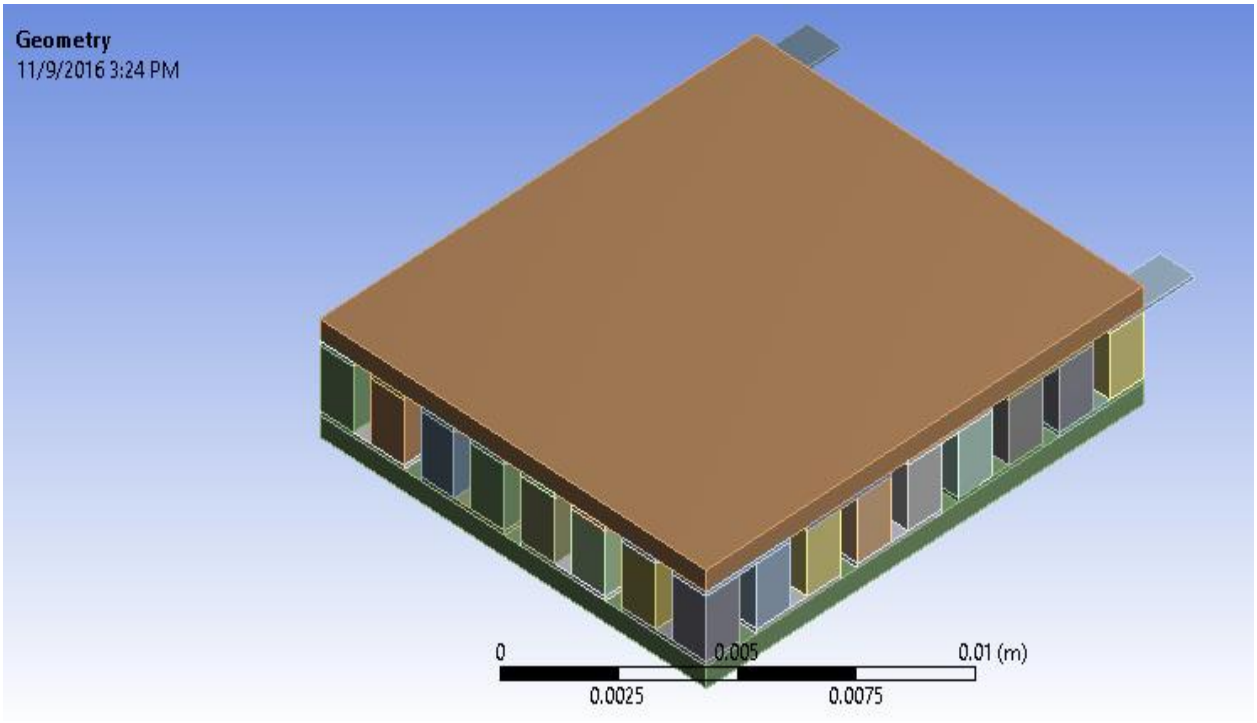

Figure 5.9 Module with 36 couples, copper and ceramic

This figure shows the geometry of the module in ANSYS. This software defines different bodies in different colors by default.in this system, we have 127 couples, copper and ceramic in the dimensions mentioned. Copper acts as an electric conductor while ceramic helps in electric insulation of the system.

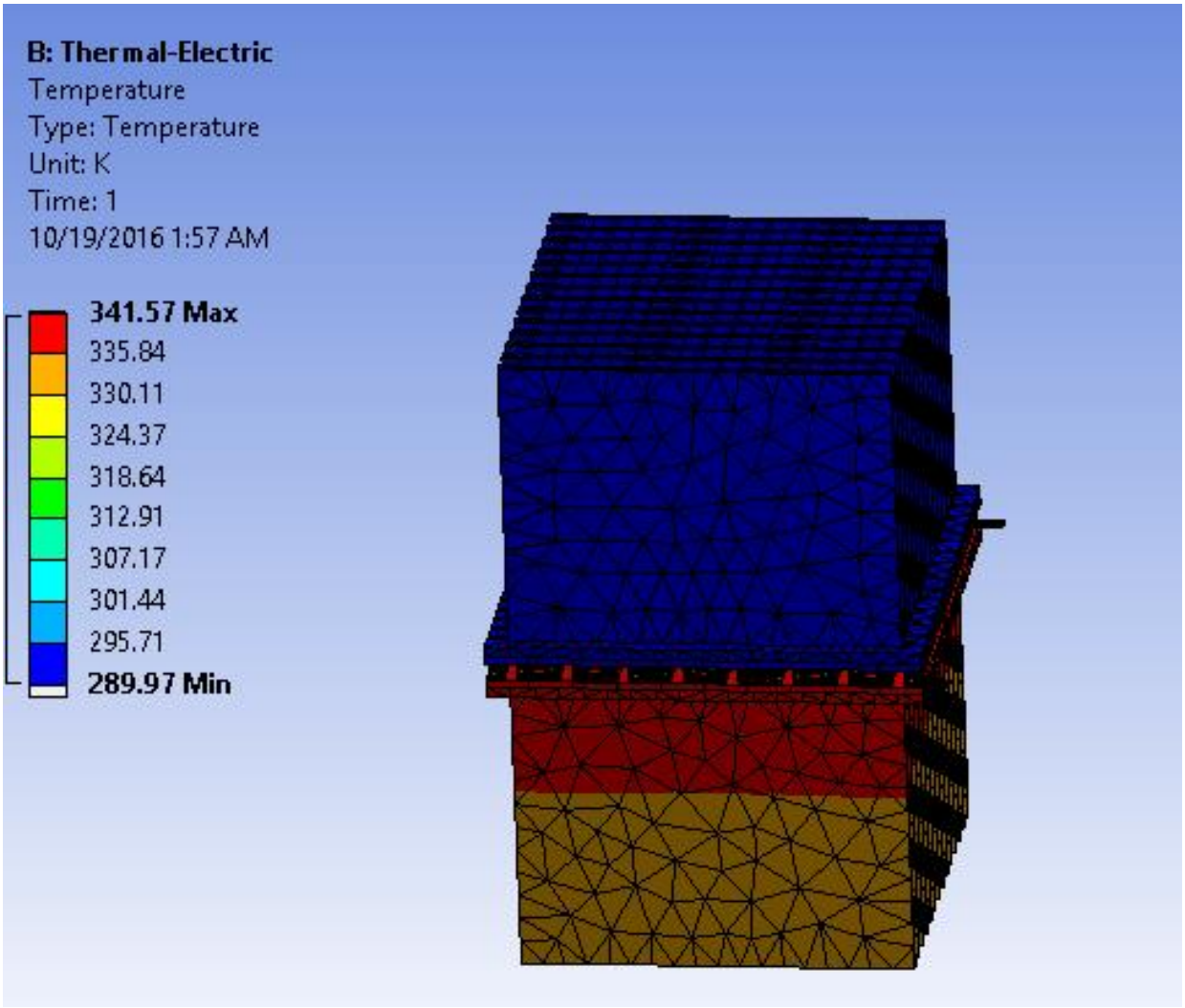

Figure 5.10 Temperature variation after CFD analysis

In order to come to this solution, using CFD, temperature inputs and mass flow rates on the cold side and hot side of the heat sink must be given as shown in Figure 4.4. Once these inputs are given and all the boundary conditions are setup, the CFD is run. And the result is shown in the figure above. Once the results have been calculated using CFD, it is integrated in the thermoelectric module as shown in

Figure 4.6. Once the integration is done and once the results of the CFD have been imported into the thermoelectric module, the module is then solved in order to calculate the cooling power on the cold side of the module. A reaction probe is set on the cold face of the module as shown in the figure below.

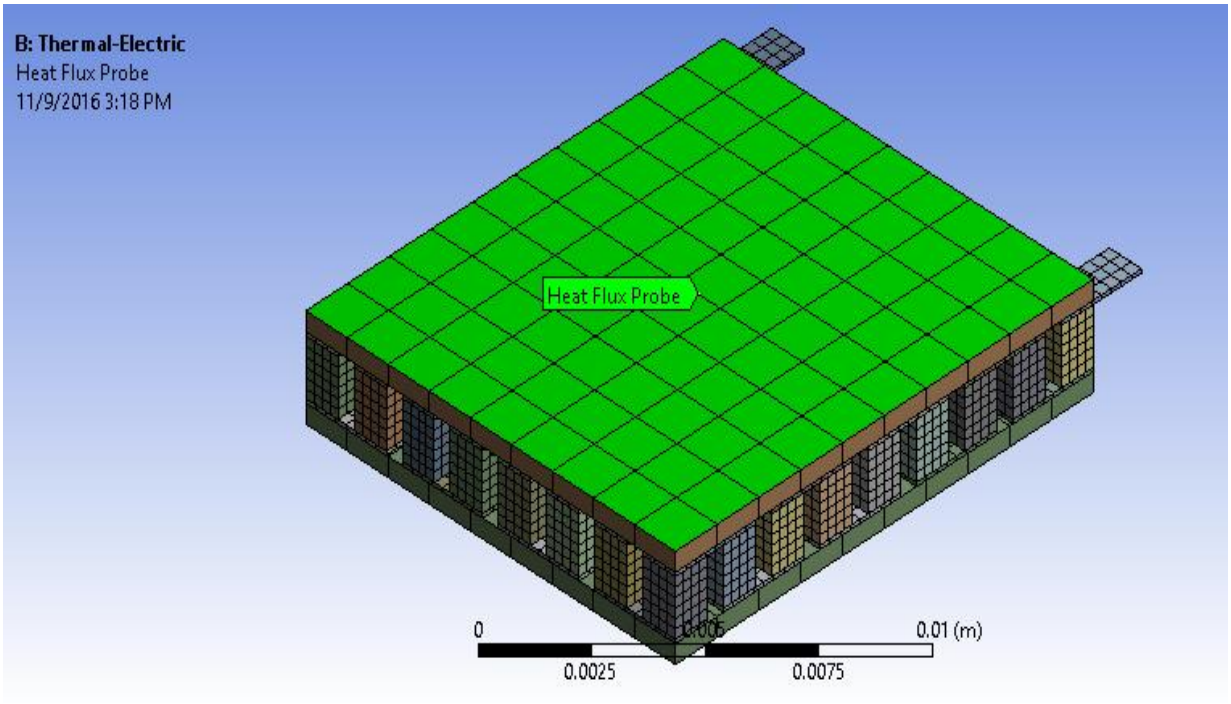

Figure 5.11 Thermoelectric module solution in ANSYS

This figure shows the probe of the heat reaction on the cold side of the module. This has been solved with respect to the results obtained from CFD. The MathCad equations have been validated using this method of simulation. In the equations, contact resistance and copper resistance have been included. When we get the results for this, it can be seen that both the methods of validation are in very good agreement with each other.

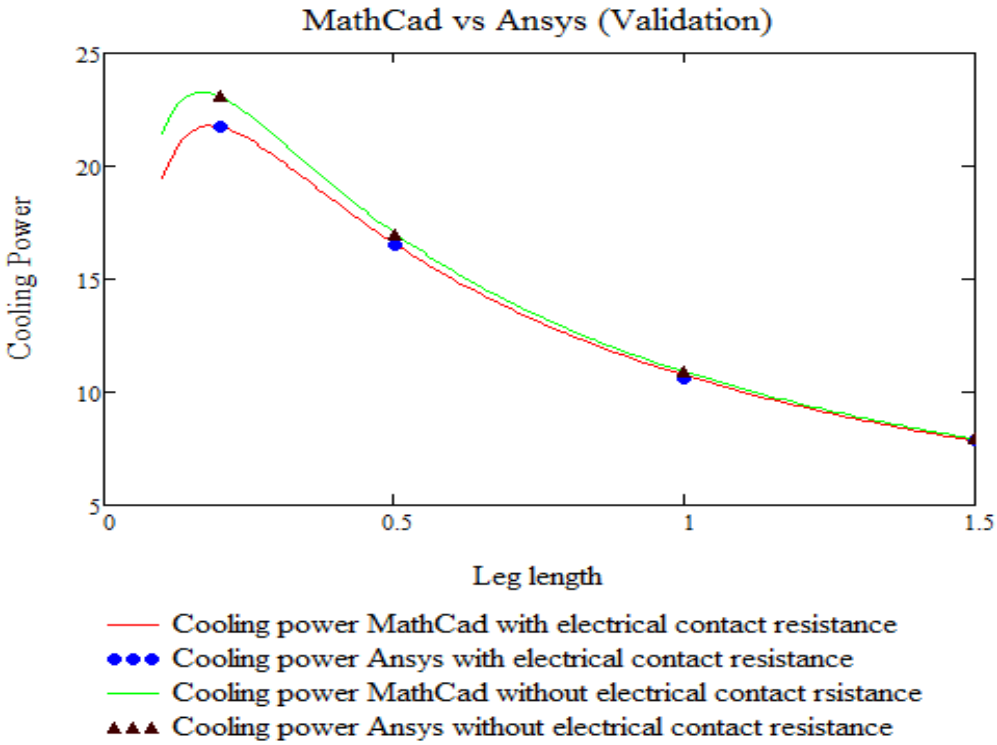

Figure 5.12 MathCad vs ANSYS for a complete module including Heat Sink

In the figure above, we can see that the cooling power predicted using analytical modeling and numerical simulation are in very good agreement with each other. There is an optimum value of leg length below which there is a drop in the cooling power. It has to be noted that, under the same conditions, the cooling power obtained in the presence of a heat sink is lower when compared the cooling power

obtained in the absence of a heat sink. This happens mainly because thermal contact increases for the heat sink material hence increasing the resistance that acts on the module. But it should also be noted that the trend that occurs in the cooling power is the same. There is an optimum leg length beyond and below which the value of cooling power cannot be maximum.

From all his discussion, the most important details that we need to note are that the electrical contact resistance effect the cooling power of a thermoelectric module at low leg lengths. However, the difference in the power obtained at these leg lengths is around 0.2W (5%). Hence, neglecting the electrical contact resistances can still predict a value closer to a real life situation.

At lower leg lengths, the copper electrical resistance is very important and there is an over prediction in the value of cooling power obtained when this resistance I obtained. The difference is cooling power is around 30W (54%). This error is way too high and it would not be correct to ignore the copper resistance at lower leg lengths, however, around 1.5mm that is the usual value of leg length for a commercial module, the effect of copper electrical resistance reduces considerably and becomes negligent. Hence at higher leg lengths, these resistances can safely be ignored.

6 Conclusion

This work was mainly aimed at validating analytical equations using numerical simulation. A lot of discussion has also been made on the importance of electrical contact resistance and electrical copper resistance. It has been found that integrating CFD into thermal electric module during the ANSYS simulation helps in deriving reliable results to validate the accuracy of the ideal equations. The discussion started off with explaining about the impact on a single module and then the same discussion was implemented on a complete module containing 36 modules. Miniature modules and macro modules were discussed and each of the parameters that impacted the overall cooling power of module was focused. The value of copper resistance and contact resistance is as such very low. But when the leg length is very low, the resistance values come in comparison with the value of the leg length. Hence, it starts impacting the cooling power and performance of the system. In higher leg lengths, however, the value of resistance is very low when compared to the value of the leg length. Hence, even though there is an impact on the cooling power, it is so insignificant that it can be neglected. Both kinds of modules have their respective applications, hence from the discussion, we can conclude that depending on the application, we can choose to select the type of module we would like to use. Also, we can safely say that numerical simulation is close to experimental validation. Since the work done concentrates on optimized modules, it is difficult to manufacture these modules according to customized dimensions. Each application needs to be optimized in a certain way and hence most of the

times, no two modules have similar dimensions. While optimizing, the modules for its input conditions end up with different optimized parameters depending on its input conditions. Modules ending up with very low leg length is very difficult to manufacture and sometimes need a new technology to build it. It is very difficult and also expensive to manufacture these kinds of modules. Hence the ANSYS simulation acts as a supplement to an experimental analysis.

7 Future Scope

- Work can be done to improve the ceramic material property. One example of a better ceramic material is Aluminum Nitride with a thermal conductivity of 180W/m*K while the ceramic used in this work is Aluminum Oxide that has a thermal conductivity of 27W/m*K.
- This study can be extended to a system with number of modules. An application can be cited in thermoelectric air conditioning system that used more than one module. This is an expensive experiment and hence can be simulated using ANSYS to get similar results. This kind of simulation however requires a high end work station that comes with a full version of ANSYS.
- The analysis done in this project ignores a lot of physics as explained in the assumption of the ideal equations. Future work can be done including such physics like the temperature dependency of the material properties, radiation heat losses and also the transfer of heat in the longitudinal direction if more number of modules are included in a thermoelectric system.

REFERENCES

[1] H. Lee, Thermoelectrics- Design and Materials, John Wiley and Sons, 2016.

[2] H. Lee, Thermal Design: Heat Sinks, Thermoelectrics, Heat Pipes, Compact Heat Exchangers, and Solar Cells, Hobooken: John Wiley & Sons, Inc., 2010.

[3] A. Attar, "Studying the Optimum Design of Automotive Thermoelectric Air Conditioning," Kalamazoo, 2015.

[4] R. DM., *Thermoelectric HAndbook: Macro to Nano,* 2006.

[5] C. G., *Nanoscale energy Transport and Conversion,* 2005.

[6] C.-Y. L. C.-I. H. Wei-Hsin Chen, "A numerical study on the perfoemance pf miniature thermoelectric cooler affected by Thomson Effect," *Applied Energy,* pp. 464-473, 2012.

[7] E. M. C. R. Simons RE, *An assessment of module coolig enhancement with thermoelectric coolers,* 2005.

[8] S. S. J. G. P.K.S. Nain, "Non-Dimensional Multi-Objective Performance OPtimization of Single Stage Themoelectric Cooler," *Springer,* pp. 404-413, 2010.

[9] C. Vinning, "An inconvenient truth about thermoelectrics," *Nature Materials,* vol. 8, no. 2, pp. 83-85, 2009.

[10] J. L. T. a. J. H. C.W. Maranville, *Improvinf efficiency of a vehicle HVAC system with comfor modeling, zonal design, and thermoelectric devices,* 2012.

[11] H. Lee, "The Thomson Effect and the ideal equation on Thermoelectric Coolers," *Energy,* vol. 56, pp. 61-69, 2013.

[12] H. Lee, Thermal Design: Heat Sinks, Thermoelectrics, Heat Pipes, Compact Heat Exchangers, and Solar Cells, Hoboken: John Wiley & Sons, Inc., 2010.

[13] H. Lee, A. Attar and S. Weera, "Performance Prediction of Commercial Thermoelectric Cooler Modules using the Effective Material Properties," *Journal of Electronic Materials,* vol. 44, no. 6, pp. 2157-2165, 2015.

[14] D. C. a. M. K. J.R. Sootsman, *New and old concepts in thermoelectric materials,* 2009.

[15] N. Junior, "Modeling a thermoeelctric HVAC System for Automobiles," *Journal of Electronic Materials,* vol. 38, no. 7, pp. 1093-1097, 2009.

[16] H. Lee, "Optimal design of thermoelectric devices with dimensional analysis," *Applied Energy,* vol. 106, pp. 79-88, 2013.

[17] T. M. Tritt, *Thermoelectric phenomena, materials and applications,* 2011.

[18] J. Sootsman, *New and old concepts in thermoelectric materials,* 2009.

[19] V. Semenyuk, *Thermoelectric Micro Modules for Spot Cooling of High Density Heat,* 2001.

[20] V. Semenyuk, *Miniature Thermoelectric modules with increased cooling power,* 2006.

[21] H. Zhang, *A general approach in evaluating and optimizing thermoelectric coolers,* 2010.

[22] H. Lee, *Optimimal design of thermoelectric devices with dimensional analysis,* 2013.

[23] H. W. CC, "Design of heat sink for improving the performance of thermoelectric generaot using two-stage optimization," *Energy,* vol. 39, no. 1, pp. 236-245, 2012.

[24] M. Makhmalbaf, "Experimental study on convective heat transfer coefficient and a vertical hexagonal rod bundle," *Heat and mass transfer,* vol. 48, pp. 1023-1029, 2012.

[25] M. Y. J. C. a. T. L. P. Teertstra, *Analytical forced convection modeling of plate fin heat sinks,* California, 1999.

[26] C. Zhimin, *The optimum design of microchannel heat sinks,* 1997.

[27] M. R. a. D. Walke, "Thermoeelctric Air Cooling for Cars," *International Journal of Engineering Science and Technology,* vol. 4, no. 5, pp. 2381-2394, 2012.

[28] M. Yamanshi, "A new approach to optimum design in thermoelectric cooling systems," *Journal of applied physics,* vol. 80, no. 9, pp. 5494-5502, 1996.

[29] X. C. Xuan, "Optimum design of a thermoelectric device," *Semiconductor Science and Technology,* vol. 17, no. 2, pp. 114-119, 2002.

[30] B. Y. Pan, "Performance analysis and parametric optimal design of an irreversible multi couple thermoelectric refrigerator under various operating conditions," *Applied Energy,* vol. 84, no. 9, pp. 992-892, 2007.

[31] A. Attar, H. Lee and S. Weera, "Optimal Design of Automotive Thermoelectric Air Conditioner (TEAC)," *Journal of Electronic Materials,* vol. 43, no. 6, pp. 2179-2187, 2014.

[32] A. Attar, H. Lee and S. Weera, "Experimental Validation of the Optimum Design of an Automotive Air-to-Air Thermoelectric Air Conditioner (TEAC)," *Journal of Electronic Materials,* vol. 44, no. 6, pp. 2177-2185, 2015.

[33] A. Attar and H. Lee, "Designing and testing the optimum design of automotive air-to-air thermoelectric air conditioner (TEAC) system," *Journal of Electronic Materials,* no. Manuscript sumbitted for publication, 2015.

[34] K.-i. Uemura, "history of thermoelectricity development in japan," *Journal of Thermoelectricity,* no. 3, 2002.

[35] N. C. S. N. C. L. J. K. C. S. Junior, "Modeling a Thermoelectric HVAC System for Automobiles," *Journal of Electronic Materials,* vol. 38, no. 7, pp. 1093-1097, 2009.

[36] D. C. D. a. L. J. Wang, "Design and Analysis of a Thermoelectric HVAC System for Passenger Vehicles," *SAE International*, Vols. 2010-01-0807, 2010.

[37] L. E. Bell, "Use of Thermal Isolation to Improve Thermoelectric System Operating Efficiency," *IEEE*, no. 21st International Conference on Thermoelectronics (2002), 2002.

[38] M. S. Raut and D. V. Walke, "Thermoelectric Air Cooling For Cars," *International Journal of Engineering Science and Technology (IJEST)*, vol. 4, no. 5, pp. 2381-2394, 2012.

[39] C.-Y. Hsu, S.-L. Li, C.-K. Liu, R.-M. Tain, H.-C. Chien, S.-F. Hsu, C.-M. Tzeng, M.-J. Dai, H.-S. Chu and J.-D. Hwang, "Non-refrigerant thermoelectric air conditioning technique on vehicles," in *Microsystems, Packaging, Assembly and Circuits Technology Conference (IMPACT), 2011 6th International*, Taipei, 2011.

[40] C. W. Maranville, J. Schneider, L. Chaney, T. Barnh and J. P. Heremans, "Improving efficiency of a vehicle HVAC system with comfort modeling, zonal design, and thermoelectric devices," United States Department of Energy, 18 10 2012. [Online]. Available: http://www1.eere.energy.gov/vehiclesandfuels/pdfs/deer_2012/thursday/presentations/deer12_maranville.pdf. [Accessed 06 11 2013].

[41] D. T. G. R. T. Barnhart, "Development of a Thermoelectric Device for an Automotive Zonal HVAC System," United States Department of Energy, 20 03 2011. [Online].

Available: https://www1.eere.energy.gov/vehiclesandfuels/pdfs/thermoelectrics_app_2012/tuesday/barnhart.pdf. [Accessed 06 11 2013].

[42] H. C. C. W. Wang CC, "Design of heat sink for improving the performance of thermoelectric generator using two-stage optimization," *Energy*, vol. 39, no. 1, pp. 236-245, 2012.

[43] P. Teertstra, M. Yovanovich, J. Culham and T. Lemczyk, "Analytical forced convection modeling of plate fin heat sinks," in *Semiconductor Thermal Measurement and Management Symposium*, San Diego, CA, USA, 1999.

[44] C. F. W. Zhimin, "The optimum thermal design of microchannel heat sinks," in *Electronic Packaging Technology Conference*, 1997.

[45] M. Yamanashi, "A new approach to optimum design in thermoelectric cooling systems," *Journal of Applied Physics*, vol. 80, no. 9, pp. 5494-5502, 1996.

[46] B. L. J. C. Yuzhuo Pan, "Performance analysis and parametric optimal design of an irreversible multi-couple thermoelectric refrigerator under various operating conditions," *Applied Energy*, vol. 84, no. 9, pp. 992-892, 2007.

[47] G.-Y. H. H.-S. C. B. Y. D.-J. Y. Cheng-Ting Hsu, "Experiments and simulations on low-temperature waste heat harvesting system by thermoelectric power generators," *Applied Energy*, vol. 88, no. 4, pp. 1291-1297, 2011.

[48] E. T. B. H. M.A. Karri, "Exhaust energy conversion by thermoelectric generator: Two case studies," *Energy Conversion and Management,* vol. 52, no. 3, pp. 1596-1611, 2011.

[49] R. DM, Thermoelectrics handbook: micro to nano, New York: Taylor &, 2006.

[50] H. S. A.Attar, "Optimal Design of Automotive Thermoelectric Air Conditioner (TEAC)," *Journal of Electronic MAterials,* vol. 43, no. 6, pp. 2179-2187, 2014.

[51] "Alpha Company Limited," [Online]. Available: https://www.alphanovatech.com/dxf/UB.pdf.